NASA CONTRACTOR REPORT

NASA CR-1073

CRYOGENIC MAGNETOMETER DEVELOPMENT

by W. S. Goree, B. S. Deaver, Jr., V. W. Hesterman, and T. W. Barbee, Jr.

Prepared by
STANFORD RESEARCH INSTITUTE
Menlo Park, Calif.
for Ames Research Center

NATIONAL AERONAUTICS AND SPACE ADMINISTRATION • WASHINGTON, D. C. • JUNE 1968

NASA CR-1073

CRYOGENIC MAGNETOMETER DEVELOPMENT

By W. S. Goree, B. S. Deaver, Jr., V. W. Hesterman,
and T. W. Barbee, Jr.

Issued by Originator as SRI Project No. PHU-5093

Prepared under Contract No. NAS 2-2088 by
STANFORD RESEARCH INSTITUTE
Menlo Park, Calif.

for Ames Research Center

NATIONAL AERONAUTICS AND SPACE ADMINISTRATION

For sale by the Clearinghouse for Federal Scientific and Technical Information
Springfield, Virginia 22151 – CFSTI price $3.00

ABSTRACT

A low field superconducting shield has been developed and used to provide stable magnetic fields of less than 10^{-6} G, maintained stable for as long as 6 days. The shield is a superconducting cylinder 91.5 cm long by 16.5 cm ID. The measured attenuation of externally applied axial field changes is a factor of 31 per shield radius.

The Meissner-effect and zero resistance property of superconductors has been used in the development of a magnetometer for measuring the absolute value of magnetic fields. This device has been used to measure fields as small as 2×10^{-6} G.

A magnetometer utilizing the unique zero resistance and quantized flux properties of superconductors has been developed and used to measure magnetic field changes as small as 5×10^{-7} G.

The dc Josephson tunneling effect has been used to construct (1) magnetometers with field sensitivity as good as 10^{-7} G, (2) magnetic gradiometers with which field gradients of 10^{-8} G cm have been measured, (3) linear displacement detectors with which displacements of less than 1500 Å have been measured, and (4) a system for measuring static magnetic susceptibility, which was used to study the time dependence of the Meissner effect in hollow tin cylinders.

FOREWORD

This is the final report on Contract NAS 2-2088 between Stanford Research Institute and the NASA-Ames Research Center (SRI Project PHU-5093). The research period covered 32 months, from 1 July 1964 to 7 March 1967. The principal investigator was Bascom S. Deaver, Jr. until September 1965. William S. Goree then was appointed principal investigator for the remaining 18 months of the project. Other participants in the research program were T. W. Barbee, Jr., H. J. Bradley, F. Chilton, V. W. Hesterman, and J. Swedlund.

CONTENTS

ILLUSTRATIONS

ILLUSTRATIONS

I INTRODUCTION AND SUMMARY

The general objective of the research program described in this report was to investigate the application of the unique properties of superconductors to instruments. The program had three specific objectives: (1) the construction of a superconducting magnetic shield with room temperature access and the use of this shield for long term stability tests of the Ames flux gate magnetometer, (2) the investigation of the use of superconducting Meissner-effect circuits as absolute reading magnetometers for measuring magnetic fields as low as 10^{-6} G, (3) the investigation of the use of superconducting quantized-flux circuits to measure magnetic fields or field changes as small as 10^{-6} G. These objectives were met as follows:

1. A cylindrical superconducting shield was constructed that was 16.5 cm ID by 91.5 cm long with an 8-cm-diameter room temperature access coaxial with the shield. Magnetic fields transverse and parallel to the shield axis could be reduced to less than 10^{-6} G at the center of the shield and maintained stable as long as the shield was superconducting. The longest test of the shield lasted about six days. During this experiment, two Ames flux gate magnetometers[1-3]* were tested for long term stability.

2. The linear field-versus-output voltage of Meissner-type modulators was used as an absolute magnetometer with sensitivities as good as 2×10^{-6} G. Studies were made of the signal-to-noise ratio as a function of applied magnetic field parallel and perpendicular to the modulator axis; operating frequency; ambient temperature at the modulator; and thermal environment, i.e., the effect of different thermal contact between the modulator and the liquid helium bath.

3. Numerous quantized-flux circuits were constructed and tested. The best of these was used to detect magnetic field changes as small as 5×10^{-7} G. This work was reported in detail in Midterm Report - October 1965 and in a published paper.[4]

We also studied Josephson tunneling junctions of the type described by Clarke,[5] and constructed magnetometers and magnetic gradiometers using the direct current characteristics of these devices. A cylindrical cavity was built to study the alternating current characteristics of the Clarke-type Josephson junction, although time did not permit completion of this study.

---

*References are listed at the end of this report.

Progress on this research contract was reported in informal reports to NASA-Ames:

- August 23, 1965: an interim report covering the long term stability test of two NASA-Ames flux gate magnetometers.[6]

- October 1965: a summary of progress made during the first 14 months of the contract period.[7] This report is very detailed and may be considered to supersede all previous reports except the August 1965 interim report discussed above.

Further results of research performed under this contract were reported in a paper published in The Review of Scientific Instruments.[4] This paper describes all of the work performed on the rotating superconducting shield and the quantized-flux magnetometers except for the optical heating experiments, which are presented in Section VII of this report.

The research effort during the last 14 months of the contract has been devoted primarily to the study of Meissner-effect magnetometers. However, other very interesting programs have received significant attention. The research program during this 14-month period can be categorized as follows:

1. Meissner-effect magnetometer.

2. Optical heating experiments with a quantized-flux modulator.

3. Josephson junctions, Clarke slug type.

4. Thermally-flushed lead superconducting shield.

These four topics, plus the magnetic shield and the quantized-flux magnetometer, are discussed in separate sections of this report. A description of the Meissner-effect magnetometer and our applications of the dc Josephson effect is given also in Reference 8.

The next section of this report presents the unique properties of superconductors that are applicable to this research program. The order of presentation in the following sections (III through VIII) is the chronological order of the discovery of the property most directly related to the application. Thus we describe the superconducting magnetic shields in Sections III and IV (zero resistance - 1911), the Meissner magnetometer in Section V (Meissner effect - 1933), the quantized-flux magnetometer in Sections VI and VII (quantized magnetic flux - 1961), and finally, the supercurrent tunneling devices in Section VIII (Josephson effect - 1963). Section IX presents a summary of conclusions and recommendations based on the overall research program described in this report.

II UNIQUE PROPERTIES OF SUPERCONDUCTORS

Several unique properties of superconductors make them useful for the measurement and control of magnetic fields. The techniques described here depend primarily on the following: zero electrical resistance, the Meissner effect, fluxoid quantization, and supercurrent tunneling.

A. Zero Resistance

The most evident property of the superconducting state is that of zero resistance, which was noticed by Kamerlingh Onnes in 1911 when he discovered superconductivity. The resistance to electrical current flow drops to zero in a fairly narrow region around the transition temperature, T_c. The narrowness of the region of temperature is typical of phase changes, and in a pure Type I superconductor, the transition is narrower than a millidegree.

In superconductors that are carrying currents, zero resistance results in behavior for all frequencies that is analogous to the high frequency behavior of normal good conductors. The currents are confined to the surface of the sample. Further, zero resistance with Maxwell's equations implies the exclusion of changes of magnetic flux

$$\frac{\partial B}{\partial t} = 0 \tag{1}$$

within the body of a superconductor.

B. Meissner Effect

An even more general magnetic field exclusion is observed in superconductors. The Meissner effect pertains to

$$\vec{B} = 0 \tag{2}$$

inside the superconductor. Equations (1) and (2) apply deep within the body of a superconductor. Near the surface, an exponential decay

$$|B(z)| = |B(0)|e^{-z/\lambda} \tag{3}$$

is observed. In Eq. (3), z measures the distance from the surface into the superconducting sample, and λ is the London penetration depth, which is typically of order 500 Å. The flux exclusion represented by Eqs. (1 to 3) is the principle behind superconducting magnetic shields. By switching a superconducting sample back and forth from superconductor to normal, the flux exclusion of Eqs. (1 to 3) can be used to measure magnetic field strengths.

C. Fluxoid Quantization

The superconducting state is a macroscopic quantum state. Thus, classical quantities such as the velocity of the current carriers, the electrons, are defined in the sense of an expectation value using the wave function for the superconducting state. Just as in the quantum behavior of atomic systems, the existence of the wave function implies various interference effects. One of these interference effects is that of fluxoid quantization. Quite analogous to the Bohr-Sommerfeld quantization condition, a superconductor obeys

$$\oint(2m\vec{v}_s - 2\frac{e}{c}\vec{A}) \cdot d\vec{x} = nh \tag{4}$$

In Eq. (4), $\vec{v}_s$ is the superconducting electron velocity, and $\vec{A}$ is the electromagnetic vector potential. The electron charge and mass are e and m, respectively. They appear as 2e and 2m due to the pairing that causes superconductivity.

In a wide variety of circumstances, one can consider a contour for this line integral that is deep within the body of a superconducting sample where $v_s = 0$. The second term of the integral is proportional to the magnetic flux,

$$\oint\vec{A} \cdot d\vec{x} = \int\nabla x\vec{A} \cdot d\vec{s} = \int\vec{B} \cdot d\vec{s} \tag{5}$$

linking the circuit. In these circumstances then, the magnetic flux is quantized (flux quantum unit = $\Phi_o = hc/2e \simeq 2 \times 10^{-7}$ G cm^2).

Flux quantization means that the only possible values of magnetic flux trapped inside a thick superconducting ring are integral multiples of $hc/2e = 2 \times 10^{-7}$ G cm^2. It is interesting that flux quantization makes it possible to produce a region in which there is zero magnetic field. If a hollow superconducting cylinder is cooled below its transition temperature in a magnetic field that produces less than half a quantized flux unit through it, a current is induced in the superconductor to cancel exactly this flux and produce the lowest quantized state, i.e., zero flux inside the cylinder. Further, the current flowing in the cylinder is a direct measure of the flux that initially existed in the cylinder, and the magnetic field can be measured without access to the volume occupied by the field and without motion of the superconductor.

D. Supercurrent Tunneling

Other manifestations of the macroscopic quantum nature of the superconducting state, with weakly coupled superconductors, have been used for a number of ingenious devices for magnetic measurements.[5,9]

Tunneling characteristics unique to the superconducting state result when two superconductors are separated by a very thin dielectric layer, approximately 20 Å, or by thin superconducting links. Direct current up to some critical value will tunnel through this junction without producing a voltage drop. This supercurrent tunneling is usually referred to as the dc Josephson effect. For currents somewhat larger than this critical value, a finite voltage appears, and high frequency current oscillations occur through the junction. This is the ac Josephson effect. The Josephson equation $h\nu = 2eV$ gives the frequency, ν, of these current oscillations versus the voltage drop, V, across the junction. In this equation, e is the charge of a single electron and h is Planck's constant. Excellent reviews of these effects are given in References 10 and 11.

The dc Josephson effect has received considerable experimental and theoretical study over the past few years and shows promise of being useful as a very sensitive instrument for measuring changes in applied magnetic field, small currents, and very small voltages. The usefulness of these junctions can best be understood by considering the equation that determines the maximum zero voltage current that can be developed across the tunnel junction.

$$I_c = I_o \left| \frac{\sin(n\pi \, \Phi_j/\Phi_o)}{n\pi \, \Phi_j/\Phi_o} \right| \qquad (6)$$

From this equation we see that the critical current, I_c (i.e., the current for which a voltage first appears) is a periodic function of the magnetic flux, Φ_j, linking the junction between the two superconducting planes with period proportional to the flux quantum, Φ_o. Further, we notice that this equation for the critical current is analogous to the equation for the amplitudes of the Fraunhofer diffraction pattern of a single slit optical diffraction grating. This pattern has a maximum at zero applied field and successive lower order maxima at integral quantum values of the flux through the junction.

In principle, a single Josephson junction exhibiting these diffraction effects can be used as an absolute magnetometer, since the critical current is a maximum for zero applied field linking the junction.

In junctions of rather large cross section area or where high tunneling currents exist, the tunnel current itself is large enough to influence the magnetic field within the junction. This effect is analogous to the Meissner effect and tends to shield part of the junction from external field changes. Because of this, junctions cannot be made arbitrarily large to gain enhanced sensitivity.

Several investigators have shown that enhanced sensitivity can be achieved by connecting two or more Josephson junctions in parallel.[9] For a circuit of two identical junctions connected in parallel, the equation for the critical current versus magnetic field is

$$I_c = I_o \left| \frac{\sin(n\pi \Phi_j/\Phi_o)}{(n\pi \Phi_j/\Phi_o)} \cos\left(\frac{n\pi \Phi_A}{\Phi_o}\right) \right| \qquad (7)$$

where Φ_j is the flux through each junction and Φ_A is the total flux linking the area between the junctions. From this equation we see the diffraction pattern given in the previous equation for a single junction multiplied by a term that is analogous to the interference term of a multiple slit optical interferometer. This interference term modulates the diffraction effect in a periodic manner where the period is now proportional to the magnetic flux, Φ_A, linking the area, A, defined by the leads connecting the two junctions. Since this area between the junctions can be many times larger (even orders of magnitude larger) than the junction area, the interference period can be much smaller than the diffraction period. Figure 1 shows an idealized current versus field plot for a double junction interferometer. We see both the diffraction envelope of a single junction and the high frequency oscillations due to the interference effect.

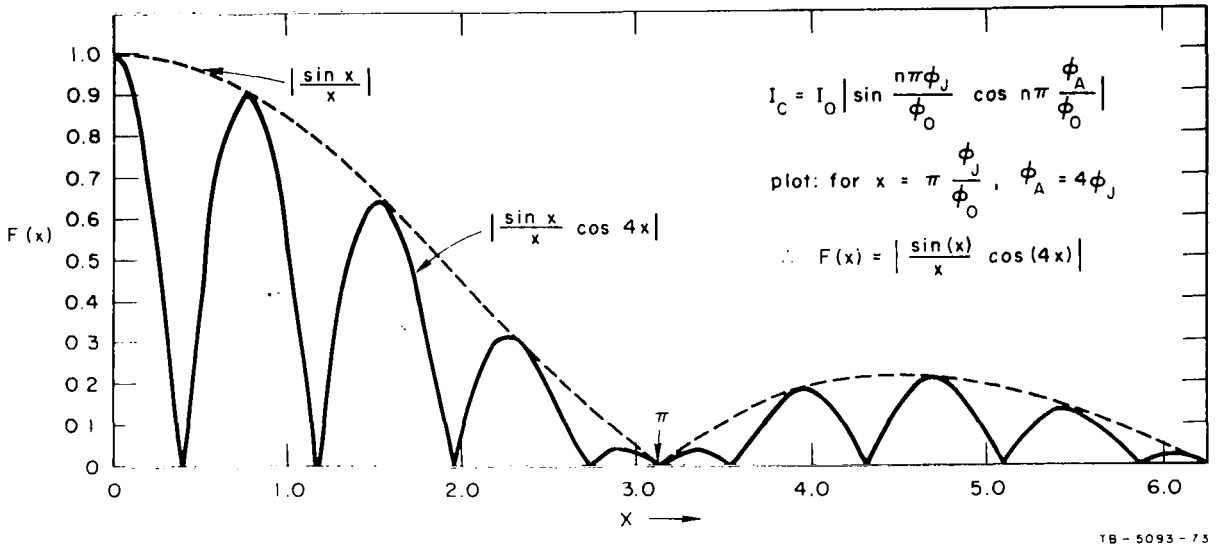

FIG. 1 IDEALIZED CRITICAL TUNNELING CURRENT VERSUS MAGNETIC FIELD FOR A DOUBLE JOSEPHSON JUNCTION INTERFEROMETER

The magnitude of the flux quantum is 2×10^{-7} G cm^2. Thus if the area between the parallel junctions is 1 cm^2, we see that the interference period may be as small as 2×10^{-7} G. If instrumentation allows resolution within an interference period, fields considerably smaller than 2×10^{-7} G can be measured. Forgacs and Warnick[12] reported sensitivities as good as 2×10^{-9} G with a double junction magnetometer.

III SUPERCONDUCTING MAGNETIC SHIELD

The superconducting magnetic shield has been described in detail in the Midterm Report of October 1965[7] and in a published paper;[4] thus only a discussion of the construction and final performance will be given here.

Sensitive devices for measuring low magnetic fields require a test region in which the magnetic field can be reduced to less than 10^{-6} G and maintained stable for many hours. For this reason, a superconducting magnetic shield was constructed and used with a combination of several techniques to achieve the low field environment. The shield structure is diagramed in Figure 2. A pair of ferromagnetic shielding cylinders fabricated of Mu-metal were used to reduce the ambient field by a factor of approximately 100. A coil wound around the inner Mu-metal shield was used to apply an alternating field to this shield to reduce fields due to permanent magnetization.

The superconducting shield was thermally isolated from the liquid helium bath so that its temperature could be varied slowly through the superconducting transition temperature. Provision also was made for rotating the shield at approximately 1 revolution/sec in order to make use of the shielding of transverse fields by the eddy-currents induced in the superconducting cylinder as described by Vant-Hull and Mercereau.[13] In this way, the transverse fields were reduced by a factor of 10^2 to 10^3. Finally, the predominantly axial field inside the superconducting cylinder was nullified with a superconducting solenoid, which was then switched to the persistent current mode to maintain time stability of the resulting low field. A superconducting transformer, connected in series with the persistent current solenoid, was used for applying precise small increments of magnetic field.

Both superconducting and room temperature devices were to be used in the low field region; therefore, a Dewar was placed inside the superconducting solenoid to provide isolation from the liquid helium bath. This inner Dewar could be filled with liquid helium or maintained at room temperature.

Special care was used in the selection of nonmagnetic materials for the construction of the apparatus. The dewars were primarily aluminum

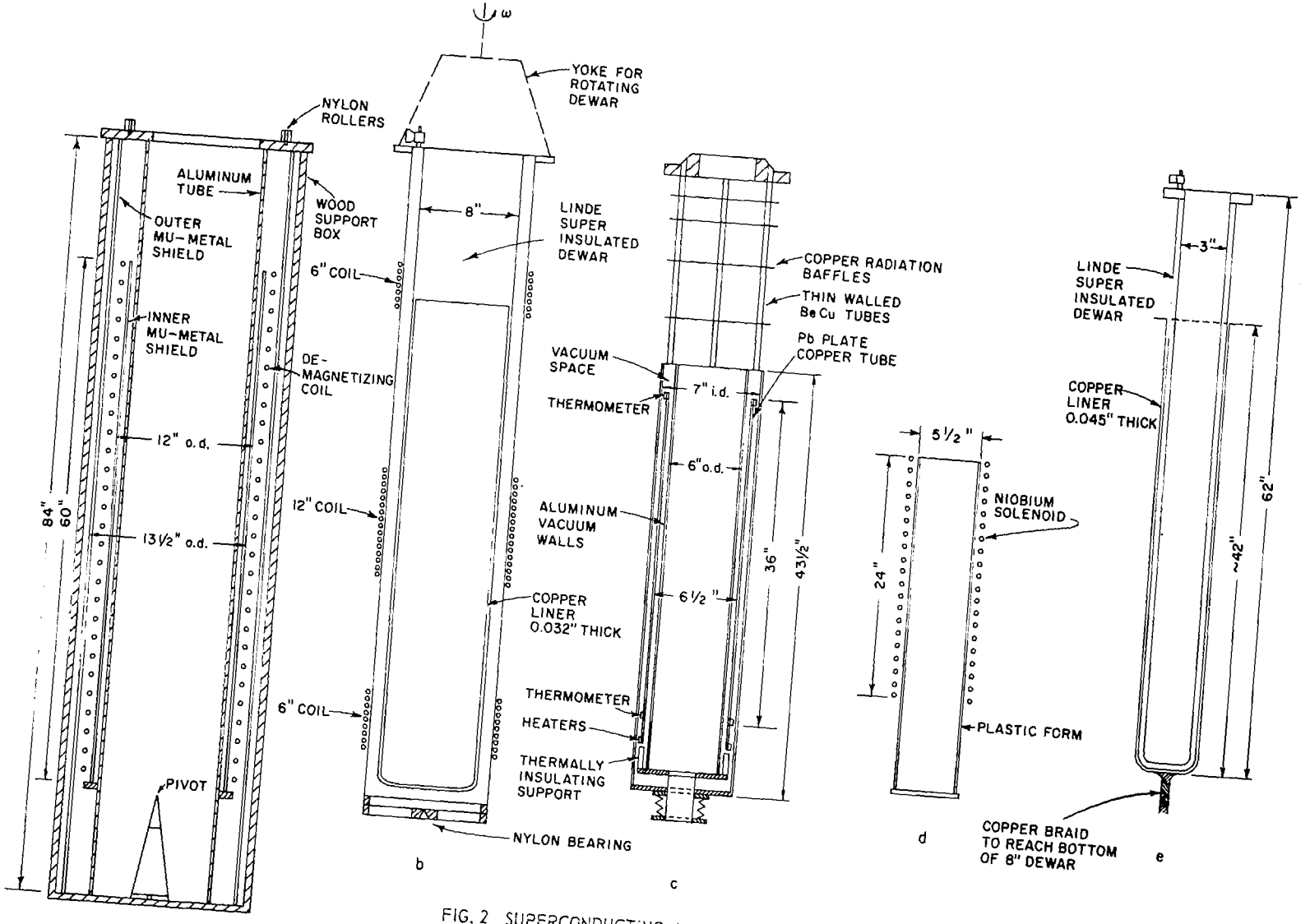

FIG. 2 SUPERCONDUCTING MAGNETIC SHIELD ASSEMBLY

TC-5093-5R

and fiberglass and required no liquid nitrogen shields.* The vacuum jacket and support structure for the superconducting shield and solenoid were also primarily aluminum with beryllium-copper tubing used for the vacuum lines from the low temperature region to the room. Nonsuperconducting cadmium-zinc solder was used, and joints between beryllium-copper tubing and aluminum were sealed with indium gaskets, which were not superconducting at the shield operating temperature.

The superconducting cylinder was a 0.013-cm-thick lead coating on the surface of a copper cylinder 91.5 cm long by 16.5 cm OD with 0.075-cm-thick walls. The superconducting solenoid, 13 cm ID and 60 cm long, was wound of 0.025-cm niobium wire. The large Dewar, containing the superconducting shield, was 20 cm ID by 210 cm long; the inner Dewar provided an 8-cm-diameter access inside the shield, which was maintained at either room temperature or liquid helium temperature.

The performance of the magnetic shield was evaluated using a flux gate magnetometer[1] designed by NASA-Ames Research Center, with which fields down to 10^{-6} G could be measured. More than 100 measurements were made of the field distribution along the axis of the shield system with the superconductors in the normal state. When the inner Mu-metal shield had not been demagnetized for a period of several days, the field along the center 1-meter length of the system was about 10^{-3} G. Immediately after demagnetizing, by subjecting the shield to alternating fields of approximately 10 G at 60 cycles and slowly decreasing this applied field to zero over a period of 100 seconds, the remaining field was found to be between 10^{-4} and 10^{-5} G. However, the field pattern was not reproducible.

The transition of the lead cylinder into the superconducting state was found to occur over a temperature interval of 0.01°K as determined by observing the change in pickup on a sensing coil inside the shield as a small ac field was applied with a solenoid external to the shield. The superconducting shield was heated approximately 0.01°K above the transition interval and then cooled through about 0.04°K over a period of 1 hour while rotating at the rate of 1 revolution/sec. When the transverse field measured on the shield axis was 10^{-3} G initially, a final field of approximately 10^{-6} G resulted, indicating an attenuation of 10^{3}. Similar attenuations may have resulted for lower initial fields, but we could not measure fields less than 10^{-6} G during the experiments. The axial magnetic field was found to be unaltered by the transition of the lead cylinder into the superconducting state.

---

* Linde Model CD-217 liquid helium hot-cold well Dewar, non-nitrogen shielded.

The Ames flux gate magnetometer was used as a null detector by first reading along one direction, flipping the probe 180 degrees, and averaging the two readings to determine the zero field; the field at the center of the shield was reduced to less than 10^{-6} G by a current flowing in the niobium solenoid, which was then switched to its persistent mode. Using these procedures, fields less than 10^{-6} G could be achieved over the center 1-cm length of the shield with gradients of approximately 10^{-6} G/cm over regions up to 30-cm long. The field at the center of the shield was measured continuously for a period of 150 hours and found not to vary by an amount detectable with the flux gate probe, i.e., 10^{-6} G. During these measurements, a small temperature sensitivity of the flux gate probe was discovered; however, when corrections were made for temperature variations, or when the probe was operated at precisely constant temperature, duplicate readings were obtained. The field at the end of the 150-hour period was measured under identical temperature conditions and found to be the same as that mapped at the beginning of the test.

The attenuation of axial magnetic fields was measured by applying a uniform axial field of 7.0 G with a large solenoid enclosing the outer helium Dewar. The measurements were made with the niobium solenoid heat switch on, because if the superconducting wire of the solenoid forms a persistent circuit, it couples to the external field near its ends and reduces the effective shield attenuation near the shield center. Figure 3 shows the measured field differences along the shield axis. A fit of the data indicates that the field inside the shield is falling as $\exp(-3.43Z/R)$, i.e., a factor of about 31 per shield radius, where Z is measured from one end of the shield and R is the shield radius. The attenuation for transverse fields was not measured quantitatively; however, it was checked qualitatively by applying a transverse field with a small solenoid across the end of the shield and found to be much smaller than for the axial case.

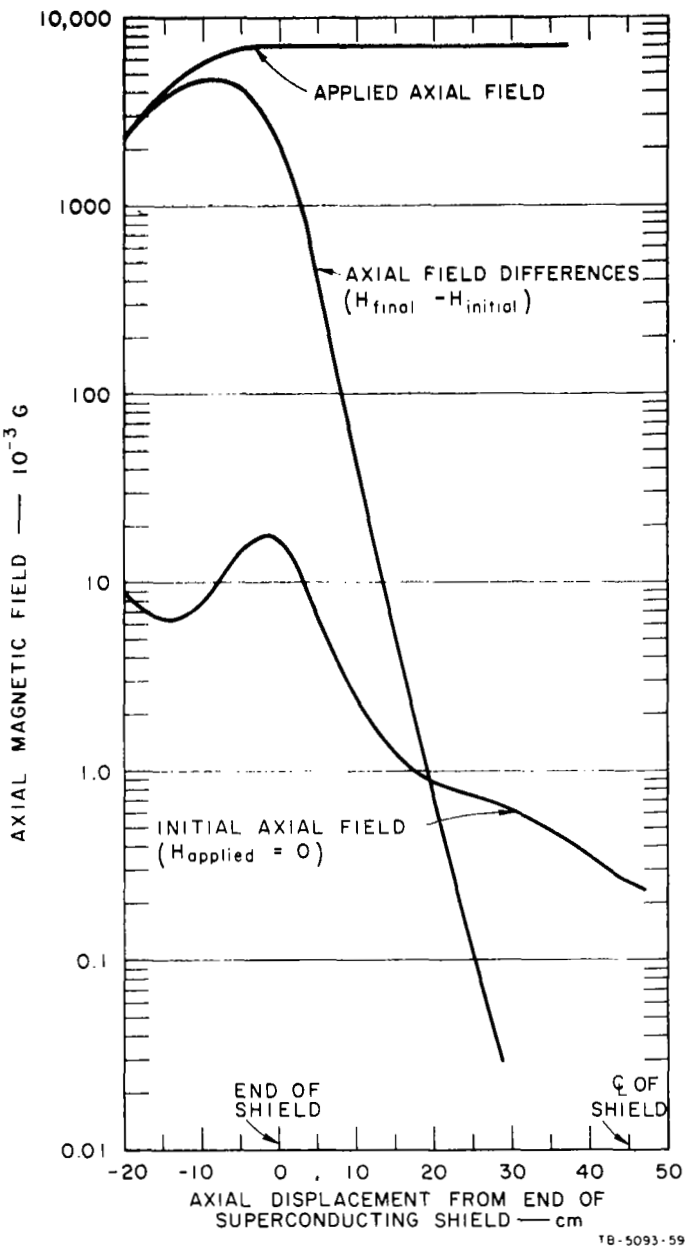

FIG. 3 ATTENUATION OF AXIAL MAGNETIC FIELD BY SUPERCONDUCTING SHIELD

IV THERMALLY-FLUSHED LEAD SUPERCONDUCTING SHIELD

Many of our experiments with both the quantized-flux and Meissner-effect magnetometers did not require the large low field superconducting system described in Section III, which was built to test the Ames magnetometers. Instead, a considerably smaller system that would use much less helium and be more convenient to work with in our experimental studies of magnetometer performance characteristics was built. It was still necessary to have a low field, stable environment for the studies, so we constructed a system suggested by Professor Hildebrandt of the University of Houston.[14] This system is essentially a closed end cylinder fitting inside a glass helium Dewar as shown in Figure 4. The cylinder is made of very pure lead welded along one seam with a spherical cap welded on one end. The outside diameter is approximately the same as the inside diameter of the helium Dewar, with sufficient clearance to allow an easy fit. To produce a low magnetic field environment, it is necessary to cool the lead cylinder through its critical temperature in a very slow and uniform fashion starting at the very bottom of the closed end. Once a small portion of the closed end becomes superconducting, we have a superconducting-normal interface propagating from this region upward to the top open end of the cylinder. If this interface is very narrow and moves slowly and uniformly, the magnetic flux within the interface will be continually pushed along and flushed out of the volume confined by the superconducting cylinder. For this system to work effectively, the interface dimensions, i.e., the distance from the point where the lead is totally normal to the point where it is completely superconducting, must be narrow enough so that large numbers of flux units are not trapped and thus locked in the volume of the cylinder.

Hildebrandt has reported field reductions of the order of 10^3 by a thermal cycle as described above.[15] In his experiments he normally mounted the lead cylinder inside a Mu-metal magnetic shield so that the ambient field was approximately 10^{-3} G and the resultant field after the thermal flush-process was 10^{-6} G.

In our experiments with a thermal-flushed shield, we were able to get field reductions of approximately a factor of 10 starting in fields of 10^{-3} G; several times we obtained a factor of 100 but never any better. We have since talked with Hildebrandt and learned that the lead used in his experiment was considerably more pure (99.9999%) than the lead we used (99.995%), which probably explains the difference in the experimental

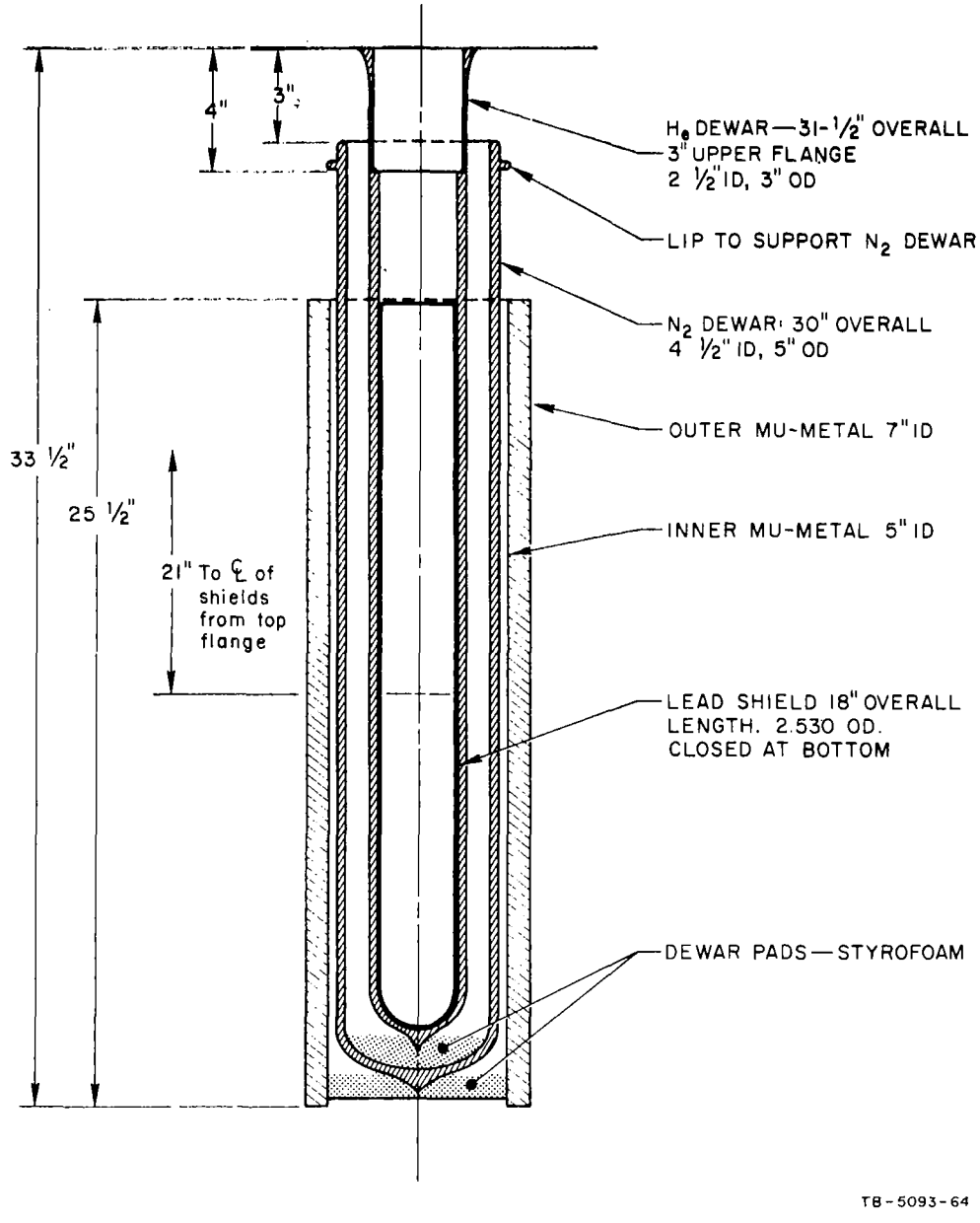

FIG. 4 THERMALLY-FLUSHED SUPERCONDUCTING SHIELD

results. The magnetic shielding characteristics of the system were not affected by this lack of adequate field reduction, and we were still able to carry out experiments inside the Mu-metal and superconducting shield.

V MEISSNER-EFFECT MAGNETOMETER

One of the major objectives of the research program described in this report was to develop an absolute reading magnetometer that does not require any preliminary calibration such as cool down in a zero field or rotating a pickup coil. Since the magnetic flux excluded by the Meissner effect is a linear function of the applied magnetic field, we undertook a detailed investigation of this unique superconducting property and its application to magnetic field measurement.

Several Meissner-effect magnetometers had already been used in some of our preliminary research.[4] The circuit used in these earlier investigations was developed at Stanford University during experiments to measure quantized flux in superconductors.[16] In this circuit, shown in Figure 5, coils A and B constitute a closed superconducting circuit; therefore the total magnetic flux linking this circuit must be constant. If the flux linking coil A is changed by $\Delta\Phi$ (for example, by removing a magnetized sample which was initially enclosed by coil A), a current is induced in the circuit, producing flux changes in A and B whose sum exactly equals $-\Delta\Phi$, thus leaving the total flux linking the circuit unchanged. The induced current will persist and is a permanent record of the flux change $\Delta\Phi$ in coil A.

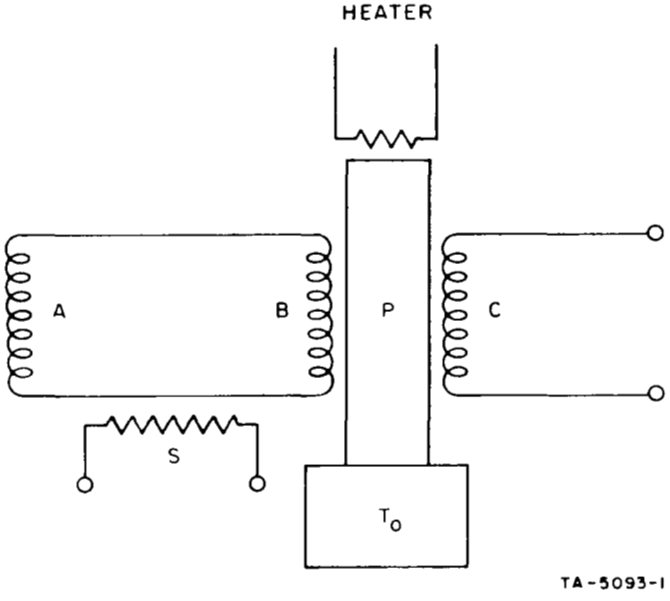

FIG. 5 BASIC SUPERCONDUCTING MAGNETOMETER CIRCUIT

Operation of the circuit to measure the persistent current, and consequently $\Delta\Phi$, is as follows: Prior to the flux change to be measured, any persistent current already present in the circuit AB is eliminated by momentarily heating a small region of the circuit with heater S, producing a normal resistance in that part of the circuit and causing the current to decay to zero. After the heat is removed and AB is again superconducting, a subsequent flux change, $\Delta\Phi$, produces a persistent current proportional to $\Delta\Phi$. A solid superconducting modulator, P, inside the pair of concentric coils, B and C, is cooled below its transition temperature through contact with a heat sink, T_o, and can be raised above its transition temperature with a heater. When the modulator is in the normal state, the current flowing in B causes flux to link B and C; when the modulator becomes superconducting, part of this flux is expelled from the modulator volume, thus changing the total flux linking B and C. When the modulator is heated and cooled periodically, the variation of flux in C produces an alternating voltage across C linearly proportional to the current in B and thus proportional to the attempted flux change, $\Delta\Phi$. Detailed circuit analysis applicable to the Meissner-effect and quantized-flux magnetometers is presented in Appendix A. (See Figure 15 in Section VI for a block diagram of the electronics generally used with these magnetometers.)

The difficulty with the solid post magnetometer circuit proved to be that the frequency response was very low, i.e., limited to about 1 kHz. This is presumably because of eddy-current damping of the flux motion over the length of the modulator and, possibly, slow thermal response. The signal power available from a circuit of this type is proportional to the operating frequency. Thus it is clear that increased output power may be obtained by increasing the operating frequency. To achieve this additional signal power, we have constructed several Meissner-type modulators that are heated internally where the thermal path is now the radial thickness of the modulator rather than its length. The modulator was cast or electroplated on a coaxial resistive heater as shown in Figure 6 and could be thermally switched at frequencies as high as 30 kHz.

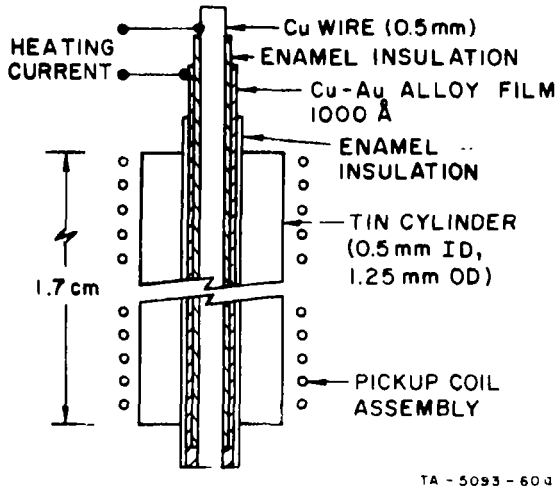

FIG. 6 MEISSNER-EFFECT MODULATOR CONSTRUCTION

A. Construction

Construction of the internally heated modulators was difficult. From the circuit analysis presented in Appendix A, we see that the signal power is directly proportional to the volume of superconductor that is switched, i.e., the amount of magnetic flux that is expelled per cycle. This, plus the fact that the Meissner effect is not nearly 100% complete, implies that a large volume of superconductor must be switched at rather high frequencies to obtain adequate signal power at very low fields, i.e., fields of the order of 10^{-6} G. In our circuits we generally have used modulators 1.25 mm OD by 0.5 mm ID by 1.7 cm long. These dimensions were arrived at to facilitate construction by calculating the electrical skin depth of the modulator material while it is still in the normal state. These calculations are presented in Appendix B. Evaporation techniques are not suitable for depositing heavy metal layers, so casting or electroplating techniques were used to form the superconducting coating. We used 99.995% pure tin for most of the Miessner-effect modulators.

Construction of the modulator heater was very similar (except for size) to that of the heaters used with the quantized-flux circuits described in Section VI. We started with an insulated copper wire, approximately 0.5 mm OD, then evaporated a copper-gold alloy heating film over the insulation that made contact to the wire at one end. It was then necessary to cover this copper-gold film with high temperature insulation so that the thick-walled superconducting modulator could be case or electroplated about the cylindrical heater. After considerable investigation we found a duPont high temperature

varnish called Pyre-ML that was suitable for dip coating, could be cured at 300°C, and would withstand temperatures as high as 300°C without deteriorating.* To insulate the heating layer, the assembly was immersed into the varnish and then extracted, using a motor drive, at about 0.1 in./sec. The assembly was cured at 150°C for 30 minutes and then baked at 300°C in an argon atmosphere for 10 minutes.

The insulated heater assemblies were then ready for the superconducting coating. If an electroplated modulator was to be used, the heater assembly was mounted in a vacuum evaporating system on a rotating fixture, and a thin layer of the metal to be plated was evaporated over the varnish. This metal layer was used as the cathode in the plating process. To ensure uniform plating thickness, the heater assembly was rotated slowly inside a cylindrical anode during the plating. The plating bath was stannous fluoroborate [$S_n(BF_4)_2$] solution as described in Reference 17. A current reversal plating procedure was used to produce more uniform platings. Current was on 18 sec and then reversed for 5 sec, etc. Using 6-ma current, about 5 hours were required to obtain a 0.35-mm wall thickness cylinder.

The casting fixture is shown in Figure 7. It is simply a quartz tube whose ID is the same as the desired modulator OD. The modulator was inserted in this tube and centered, using small standoffs made of masking tape. A rubber suction bulb was fitted to the upper end of the tube and the lower end was dipped into the molten tin bath. Tin was then drawn up into the tube with the suction bulb to the desired height and allowed to cool. Generally the slight contraction of the tin on cooling was sufficient to allow easy removal of the modulator from the quartz tube.

Modulator construction was not very reproducible. It was difficult to control the precise length of the superconducting cylinder and also to keep the heater wire centered in the casting tube. We were able to get one symmetric modulator of the correct length however, and this modulator was used in most of our experimental studies of the Meissner-effect magnetometer.

B. Experiments and Results

The purpose of these studies of the Meissner-effect magnetometer was to determine how the magnetic field sensitivity, frequency response, or

---

* Information on duPont "Pyre-M.L." is available from E. I. duPont de Nemours and Co., Fabrics and Finishes Department, Insulation Sales, 7250 N. Cicero Ave., Lincolnwood, Chicago, Ill. 60646

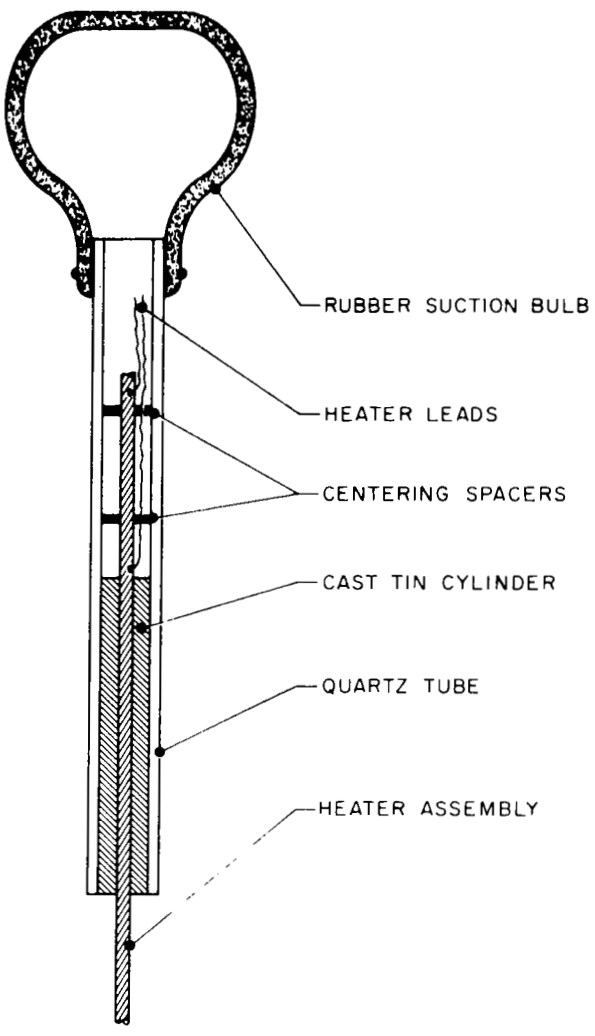

FIG. 7 FIXTURE FOR CASTING MEISSNER-EFFECT MODULATORS

signal-to-noise is affected by the magnetic and thermal environment of the modulator and thereby maximize the sensitivity to magnetic fields.

The thermal environments studied were: (1) the modulator mounted directly in the liquid helium bath, (2) the modulator mounted in a vacuum container filled with helium exchange gas and immersed in the liquid helium bath, (3) the modulator and pickup coil assembly coated with a 0.3-mm layer of silicone vacuum grease, and (4) the modulator and pickup coil assembly mounted in a 3-mm-ID by 4-mm-OD quartz tube filled with silicone vacuum grease.

The output signal for the modulator mounted directly in the liquid helium bath had a random low frequency amplitude fluctuation as shown on Figure 8. This fluctuation was similar in appearance to cryotron noise observed by Johnson and Chirlian,[18] which they associated with boiling liquid helium at the surface of the cryotron. Maximum field resolution with this modulator was about 8×10^{-6} G.

The modulator was next mounted in a helium exchange gas environment to eliminate the possibility of boiling at the modulator. Figure 9 shows a typical response trace. The low frequency noise was greatly reduced, but the frequency response also was reduced so increased field resolution was not obtained.

Next, the modulator was uniformly coated with a 0.3-mm layer of silicone vacuum grease and mounted directly in the liquid helium, Case 3. This uniform coating over the modulator and pickup coil certainly would prevent gas bubbles from forming in direct contact with the modulator and should reduce temperature gradients along the length of the modulator. The circuit response, field resolution, and noise were identical to Case 1 where the modulator was mounted directly in the liquid helium bath. This indicates that the silicone vacuum grease is an excellent thermal conductor and that the low frequency noise probably is due to temperature gradients at the modulator.

The modulator assembly was mounted in a 3-mm-ID by 4-mm-OD by 4-cm-long quartz tube that was sealed at both ends to provide further isolation from the liquid helium bath, Case 4. The circuit response for this case was almost identical to that for Case 2. The heavy wall quartz tube plus the space between the modulator and the tube account for this similarity.

These experiments indicate that the magnetometer was sensitive to thermal environment and that a low frequency noise contribution was due to helium boiling in contact with the modulator. Reducing this low frequency noise by altering the thermal environment did not measurably improve the magnetic

FIG. 8 NOISE IN OUTPUT FROM MEISSNER EFFECT MAGNETOMETER MOUNTED IN LIQUID HELIUM BATH

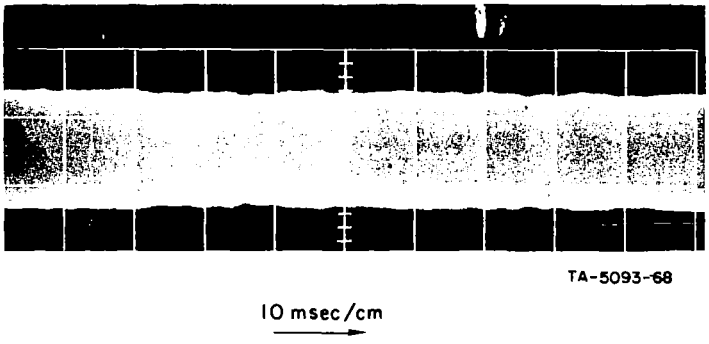

FIG. 9 NOISE IN OUTPUT FROM MEISSNER-EFFECT MAGNETOMETER MOUNTED IN HELIUM EXCHANGE GAS

field sensitivity. As will be discussed later in this section, transverse field at the modulator and eddy-current noise appear to limit the sensitivity much more than does helium boiling.

All of the above thermal environment experiments were conducted in the Dewar assembly discussed in Section IV. The modulator was mounted with its axis parallel to the Dewar and shield axis. The ambient magnetic field in this axial (vertical) direction was measured by determining the applied field required to null the output signal from the magnetometer. This field varied from about 10^{-5} to 10^{-3} G for different experiments. During these experiments we observed that the signal-to-noise ratio, measured at the null signal point, seemed to be related to the initial axial field.

The next series of experiments was designed to study the effect of magnetic fields on magnetometer sensitivity. The fields, axial and transverse to the Mu-metal shield, were measured and found to be of the same order of magnitude for different demagnetization procedures. Further, if we assume that the thermal-flushing process would reduce these initial fields by approximately equal amounts, then the transverse field at the modulator should be of the same order as the initial axial field. Thus, it appeared that transverse fields may be a significant source of modulator noise or extraneous signal.

A conclusive experimental test of this assumption was difficult in the small cryostat due to limited space for coils to control all three field components. Therefore, the large rotatable superconducting shield was used. The modulator was mounted as shown in Figure 10. The initial magnetic field components at the modulator were measured to an accuracy of $\pm$ 2 x 10^{-6} G using the Ames flux gate magnetometer and were zero parallel to shield axis. The maximum field perpendicular to the shield axis was 1.2 x 10^{-5} G. The perpendicular field also was uniform over the magnetometer dimensions. The modulator was mounted with its axis along this maximum perpendicular field and on a fixture that could be rotated by $\pm$ 150 degrees in a plane at right angles to the shield axis. The field transverse to the modulator (i.e., along the shield axis) was controlled with the persistent current niobium solenoid described in Section III. The field parallel to the modulator was controlled with a copper wire solenoid wound around the fixture holding the modulator. The third orthogonal field component was set at approximately zero by rotating the modulator until it pointed in the maximum field direction.

The results of these studies of the effect of fields applied transverse to the modulator axis are shown in Figure 11. It is clear that the noise is essentially a linear function of transverse field except at very low fields, i.e., fields low enough to produce only a few flux quanta through the transverse projected area of the modulator. The scatter of

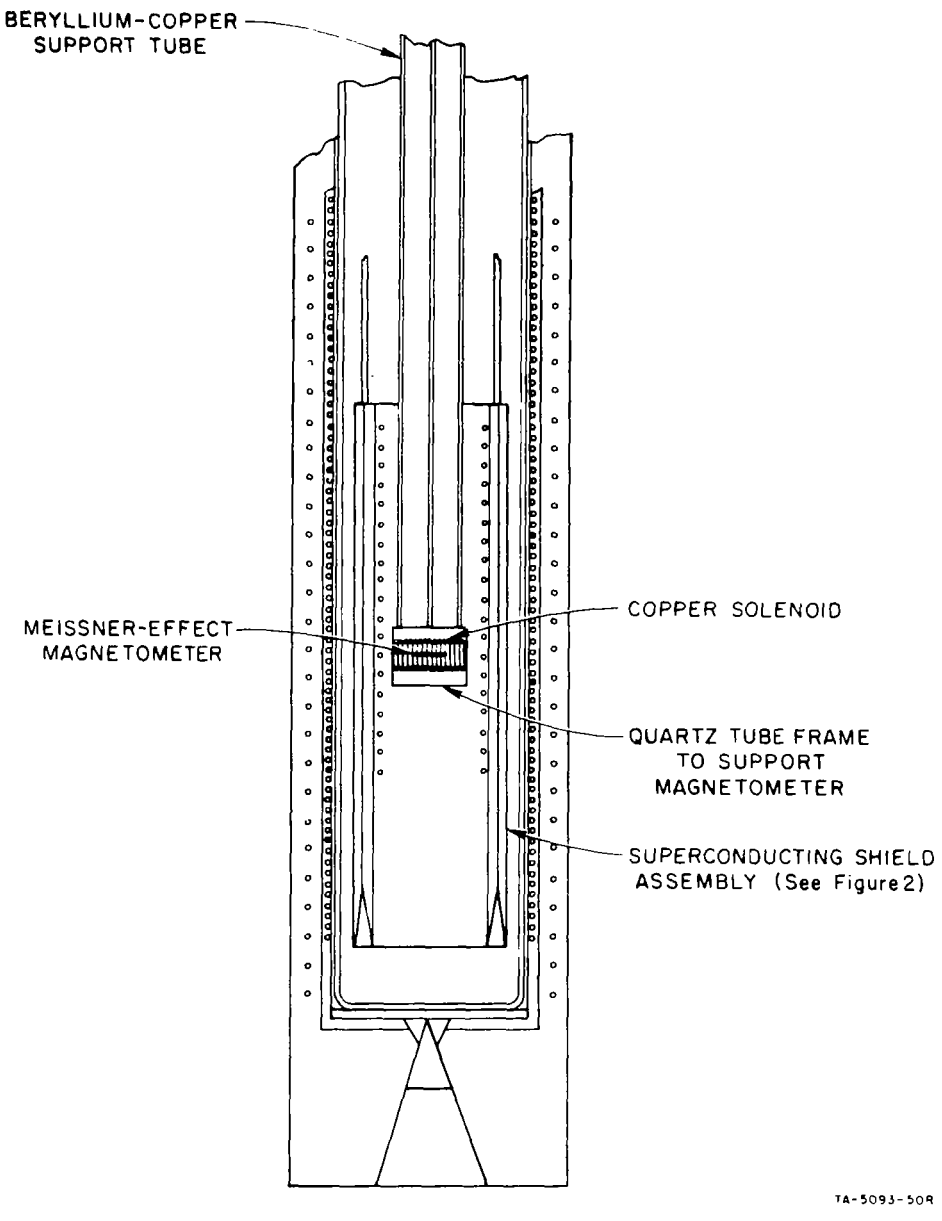

FIG. 10 MEISSNER-EFFECT MODULATOR MOUNTED IN THE 16.5-cm-DIAMETER SUPERCONDUCTING SHIELD

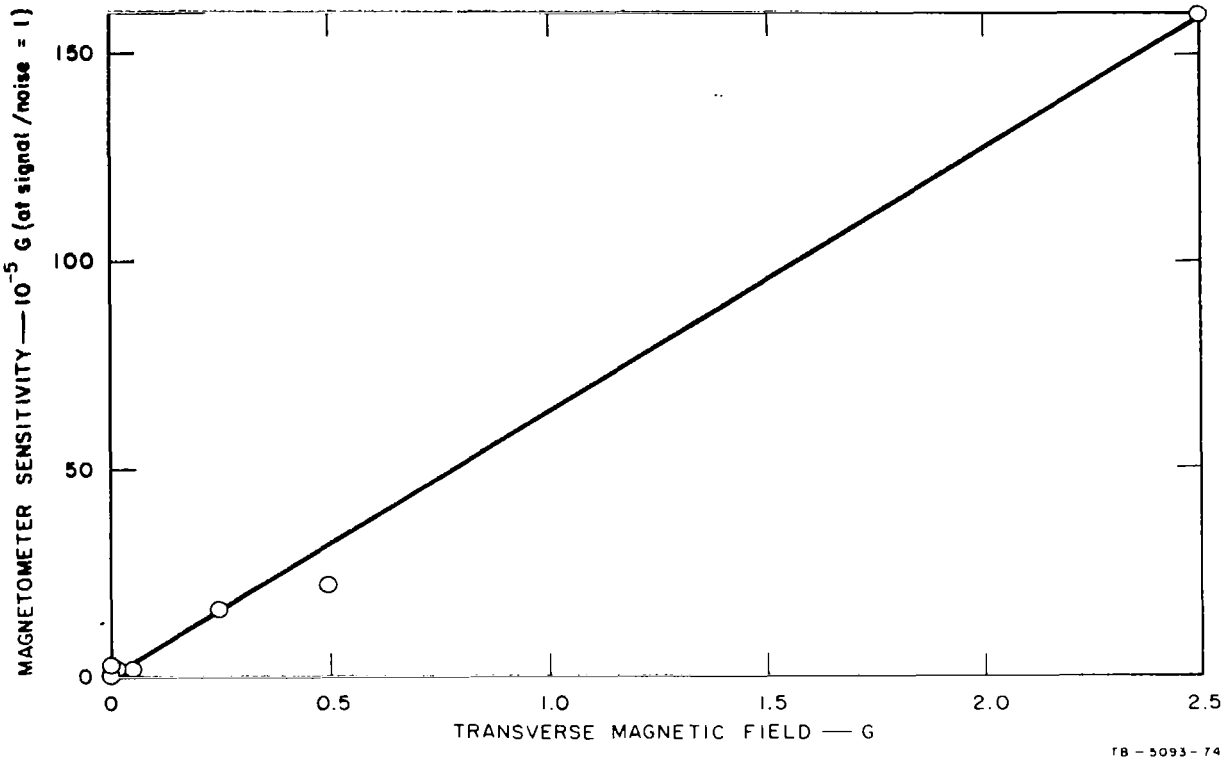

FIG. 11 MAGNETOMETER SENSITIVITY VERSUS TRANSVERSE MAGNETIC FIELD

points at very low fields probably indicates that the field was not completely uniform at the modulator, possibly due to magnetic moments of the magnetometer fixture. Also signals at these low fields were of the same order as the inherent noise in the detection circuit.

A series of measurements was made of the modulation efficiency versus heating frequency. For dc heating, the modulation efficiency is directly proportional to the change in self-inductance of the pickup coil when the modulator becomes superconducting. If the modulator is perfectly coupled to the pickup coil, the self-inductance will go to zero when the modulator becomes superconducting. To measure this coupling or modulation efficiency at higher frequencies, a 10-kHz field was applied to the modulator-pickup coil assembly with an external solenoid. The modulator was then switched with the resistive heater at a lower frequency. The output from the pickup coil was displayed on an oscilloscope. The signal from the applied field was amplitude modulated by the superconducting modulator at twice the heating frequency. The modulation efficiency is then given by $(e_{max}-e_{min})/e_{max}$,

where e_{max} and e_{min} are the maximum and minimum peak-to-peak values, respectively, of the modulation envelope as shown in Figure 12.

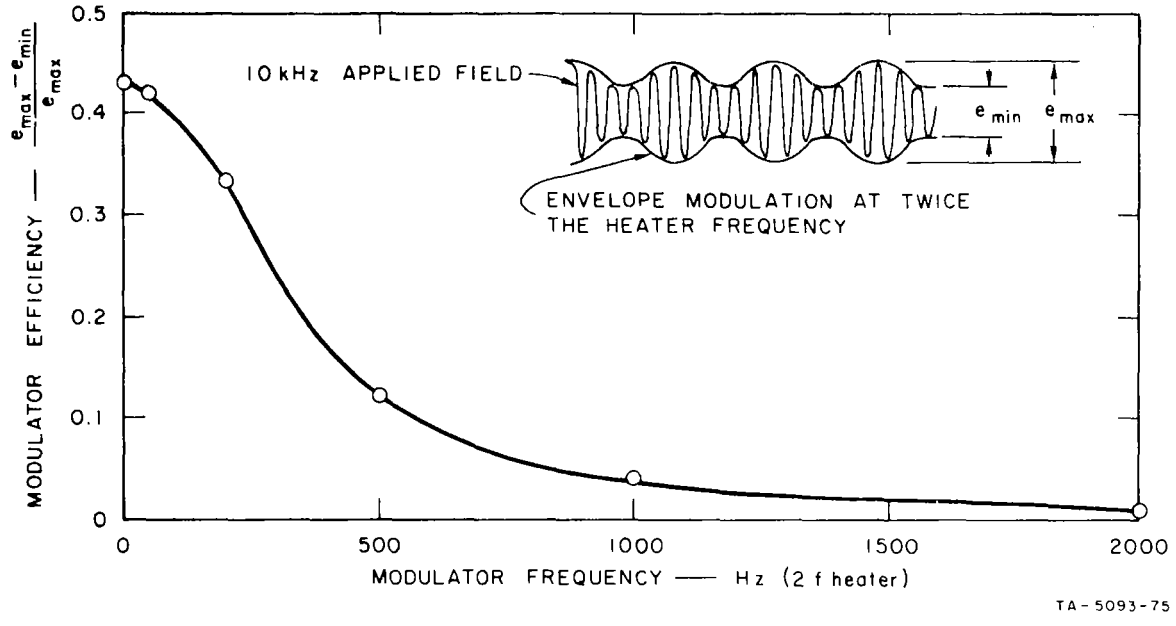

FIG. 12 MODULATION EFFICIENCY VERSUS OPERATING FREQUENCY FOR A MEISSNER-EFFECT MODULATOR

It is very important to note that the modulator efficiency measured in the manner described above is not the same as the efficiency with which flux is excluded and admitted to the modulator volume by switching in dc fields. In the measurements as described, we were measuring the change in inductance of the pickup coil as a function of modulation frequency, and this depends only on the shape and extent of the outer superconducting sheath during the switching process, since material inside this sheath is almost perfectly shielded from the coil. It does not matter how efficiently magnetic flux has been expelled from the volume inside this sheath. These data do provide an upper limit on the modulation efficiency expected for switching in steady fields.

During all of the experimental studies on the Meissner-effect magnetometer, we made checks of the dependence of the magnetometer sensitivity versus bath temperature (down to about 1.5°K) and heating pulse shape. The bath temperature did not significantly affect modulator performance except that additional heater power was required as the bath temperature was reduced. The heating pulse shapes used were generally sine wave. We tried

square wave heating on several experiments and, while magnetic field sensitivity was not improved, this method of heating did provide more control over the heating and cooling cycles. It also provided a measure of the rise time of the heating and cooling pulses. A scope photograph of the heating pulse and the magnetometer response using an untuned detection circuit is shown in Figure 13. The pulse width of the output due to heating the modulator above its critical temperature is about 0.075 msec, while the cooling pulse width is about 0.5 msec. Further, the heating output pulse can be controlled to some extent by changing the amplitude of the heating signal. The cooling pulse width, on the other hand, is basically fixed by the modulator geometry (eddy-current paths) and the thermal environment.

From the above studies of the Meissner-effect magnetometer, we can conclude that: (1) fields as small as 10^{-6} G can be measured; (2) the major noise source is the eddy-currents in the modulator that impede flux motion during the transition between the normal to the superconducting states; (3) additional noise is caused by helium boiling in contact with the modulator; and (4) signal-to-noise ratio is a function of the transverse magnetic field at the modulator. Sensitivity to axial field changes usually is not better than several orders of magnitude less than the total transverse field at the modulator.

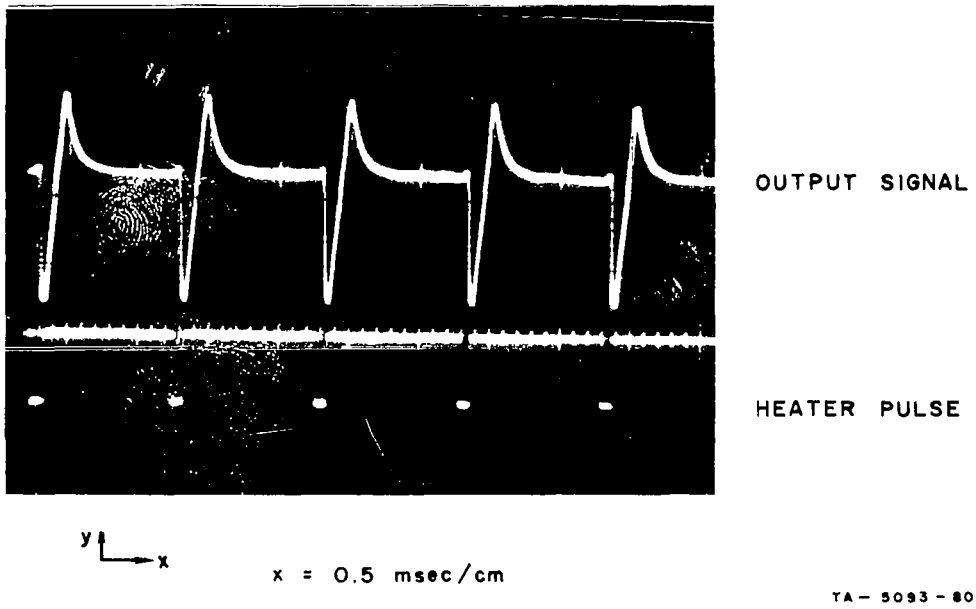

FIG. 13 OUTPUT SIGNAL FROM MEISSNER-EFFECT MAGNETOMETER FOR SQUARE-WAVE HEATING

VI QUANTIZED-FLUX MAGNETOMETER

The quantized-flux magnetometer has been described in detail in the Midterm Report - October 1965[7] and in a published paper,[4] thus only a brief discussion of the operating principles and final performance will be given here.

Quantized flux modulators (which are hollow, thin-walled superconducting cylinders) have been found to switch in and out of the superconducting state at frequencies as high as several megahertz.[19,20] With this type of modulator, the voltage across coil C (Figure 5) is a periodic function of the flux change, $\Delta\Phi$, as shown in curve (b), Figure 14. When the magnetic field in coil B, due to the persistent current in the circuit AB, produces exactly one flux unit (or any integral multiple of one flux unit) through the hollow superconducting cylinder, no flux change occurs when the cylinder is cooled through its superconducting transition. This condition gives the points of zero output shown on the response curve; however, for other values of the field, current is induced in the walls of the cylinder as it becomes superconducting to change the enclosed flux to the nearest quantized value. When the cylinder is cooled in a field producing less than one-half flux unit within it, a current is induced to oppose the applied field and produce zero flux inside the cylinder. If the cylinder is cooled in a field producing slightly more than one-half flux unit, the induced current produces a field in the same direction as that of the applied field to change the total flux to one unit inside the loop. This change gives an output voltage through coil C, opposite in sign to that of the previous case. The pattern repeats as the applied field is increased, giving an output voltage that is a periodic function of the field applied to the cylinder and thus of $\Delta\Phi$, the flux change in coil A.

The idealized response, shown in Figure 14, ignores the Meissner effect of the walls of the cylinder. In general, the response of the hollow modulator will be the periodic effect shown in Figure 14, superimposed on the linear output due to the Meissner effect of the walls. An estimate of the signal power, P_s, available from the circuit, if L_2 is a solenoid of length ℓ and area A, is given by

$$P_s \simeq (1/8\pi)\Phi^2(\ell/A)\nu, \quad \Phi < 10^{-7} \text{ G cm}^2, \tag{8}$$

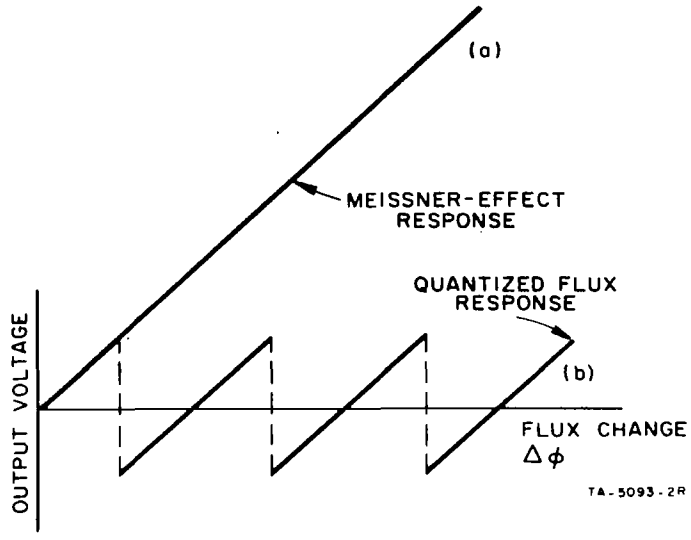

FIG. 14 RESPONSE OF SUPERCONDUCTING CIRCUIT

where Φ is the flux in L_2, and ν is the frequency at which the modulator is operated. The sensitivity of the measurement can be enhanced by using the circuit of Figure 5 with coil A replaced by a single loop pickup coil of large area (Figure 15). This device can be used in two ways: if the field penetrating the single loop produces less than one-half a flux unit through the loop (assuming zero field at coil B), then when the superconducting circuit is completed, a current will flow to expel all the magnetic flux. A measurement of this current thus constitutes a measurement of the total magnetic field. If the field produces many flux units through the loop, there is an uncertainty by the first method, since the current flowing will be proportional to the amount by which the total flux differs from the nearest integral number of flux units. In principle, one could use a series of loops of various sizes to determine the absolute field; in practice, it is simpler to move the pickup loop in the field as with a standard flip coil. Thus, by rotating the coil 180 degrees, a flux change in the loop, corresponding to twice the total field along the initial direction, causes a persistent current proportional to that field; a measurement of this current measures the field.

Since the field at the modulator enclosed by coil B (Figure 15) can be increased from that through the pickup loop by about a factor $(n_1/n_2)(A_1/A_2)$ (where n_1 and n_2 are the numbers of turns on the pickup coil and coil B, respectively, and A_1 and A_2 are their areas), a sensitivity of 10^{-6} G per period can be readily obtained. Furthermore, it is possible to resolve a small fraction of a flux unit; thus very small fields can be measured.

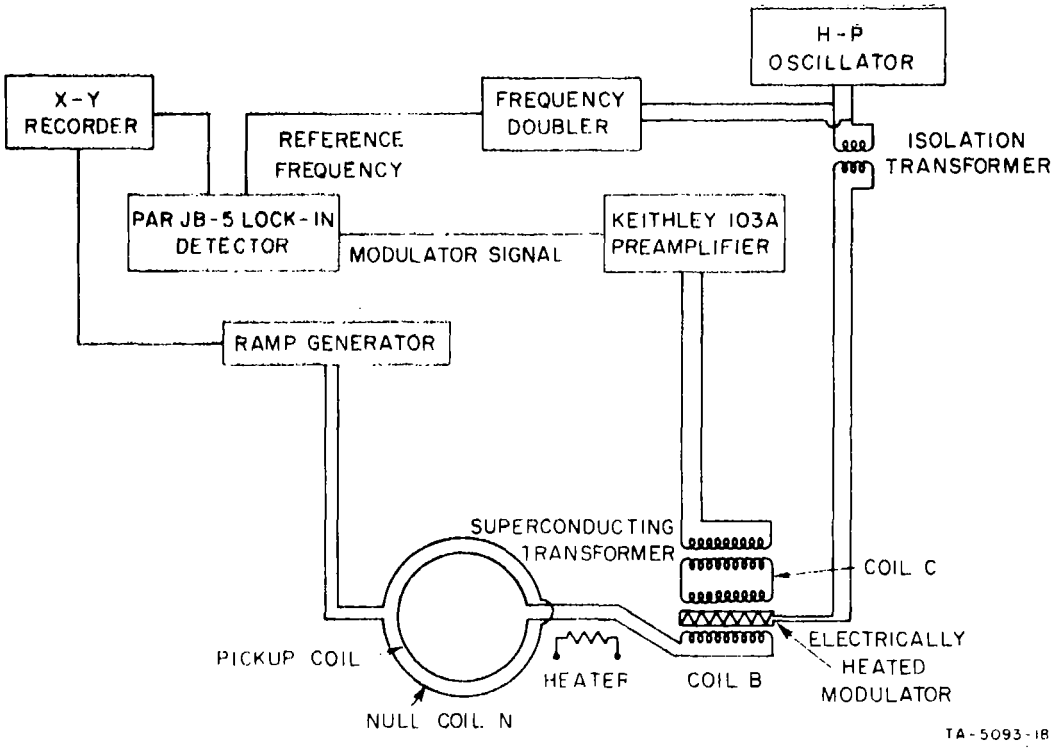

FIG. 15 QUANTIZED-FLUX MAGNETOMETER CIRCUIT

Several magnetometer circuits of this quantized-flux type have been constructed. The superconducting modulator was an indium cylinder 1 cm long with 40 μ ID and walls about 1 μ thick. It was formed by evaporation onto a coaxial heater unit fabricated by evaporating a copper-gold alloy film onto an insulated copper wire. The film contacted the copper wire at one end so that current could be passed through the wire and back through the film, thus producing heat in the resistive film. These modulators normally were switched in and out of the superconducting state at 30 to 40 kHz.

The pickup coil (Figure 15) consisted of a 1-cm-diameter single turn of 0.005-cm-diameter niobium wire connected to a coil of the same wire wound about the indium cylinder. The modulator was mounted with its axis parallel to the plane of the pickup coil and along the rotation axis of this coil when it was used as a flip coil. The trim coil was used to produce zero net flux through the modulator when no persistent current was flowing in the circuit. A superconducting transformer with an externally tuned secondary was used to match the low impedance output coil (coil C, Figure 15) to a low noise preamplifier and then to a JB-5 Princeton Applied Research lock-in detector. A coil N, closely coupled to the pickup

coil, was used to produce an opposing field charge so that the device was used as a null detector where the current flowing in coil N was a measure of the field.

The response of the magnetometer to a slowly increasing magnetic field is shown in Figure 16, where both the quantized-flux periodicity and the average linear variation due to the Meissner effect of the cylinder walls are evident. The data in Figure 16 indicate a noise limitation of approximately 5×10^{-7} G.

The operating characteristics and magnetic field sensitivity of the quantized-flux magnetometer usually become worse after several cycles to room temperature. We feel that more refined evaporation techniques would eliminate this problem.

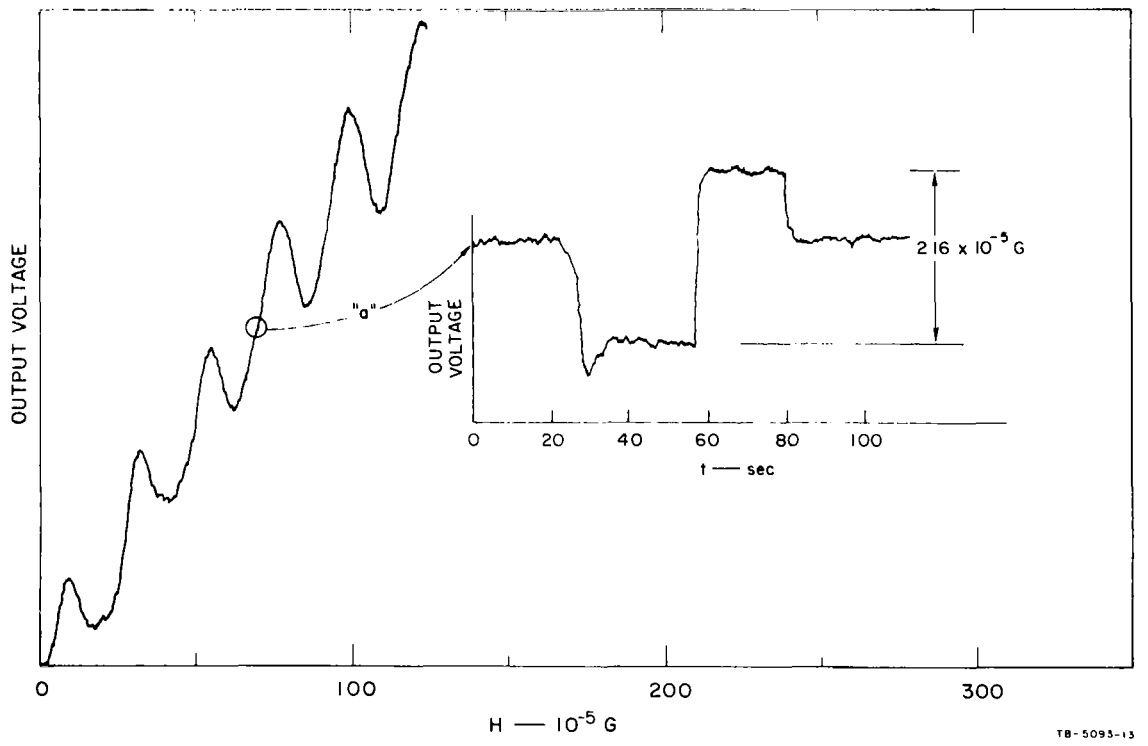

FIG. 16 QUANTIZED-FLUX MAGNETOMETER RESPONSE

VII OPTICAL HEATING EXPERIMENTS WITH A QUANTIZED-FLUX MODULATOR

The quantized-flux magnetometer has been described in the previous section and in References 7 and 4. The superconductor was heated above and cooled below its transition temperature by passing an alternating current through a resistive film coaxial with the modulator. The output signal was at twice the heater frequency since a heating pulse and a cooling pulse occur twice for every cycle. This minimizes electrical pickup between the heater and the output signal at the signal frequency, although any second harmonic content in the heater signal can still cause noise or background on the modulator output.

We designed an experimental system to test optical heating of the superconducting film in an attempt to eliminate this source of extraneous signal. This system, shown schematically in Figure 17, consists essentially of a modulator or superconducting cylinder evaporated onto a quartz fiber. Light is piped into the cryostat through a quartz light pipe and impinges on one end of this quartz fiber. The fiber is constructed in the shape of a collimator to collect more light from the light pipe. The light source is a high intensity arc lamp mounted in the room and focused by various lenses on the mirror of a Honeywell microgalvanometer.* The galvanometer is of the type used in optical strip-chart recorders. Its rated frequency response can be as high as 15 kHz and possibly higher for very low amplitude oscillations.

The complete system consists of a chopped light beam passing through the light pipe into a quartz tube onto which the modulator is evaporated. The light is absorbed by the modulator, which heats the superconductor above its transition temperature. In this system, direct coupling of the heater supply current to the modulator output circuit is avoided completely.

We constructed several superconducting modulators evaporated on quartz and tried this optical modulation experiment numerous times. All of the experiments were unsuccessful because the evaporated film on the quartz fiber would not become superconducting. Careful inspection of the modulator under a microscope showed numerous hairline cracks running axially

---

* Honeywell, Denver Division, 4800 E. Dry Creek Road, Denver, Colorado 80217.

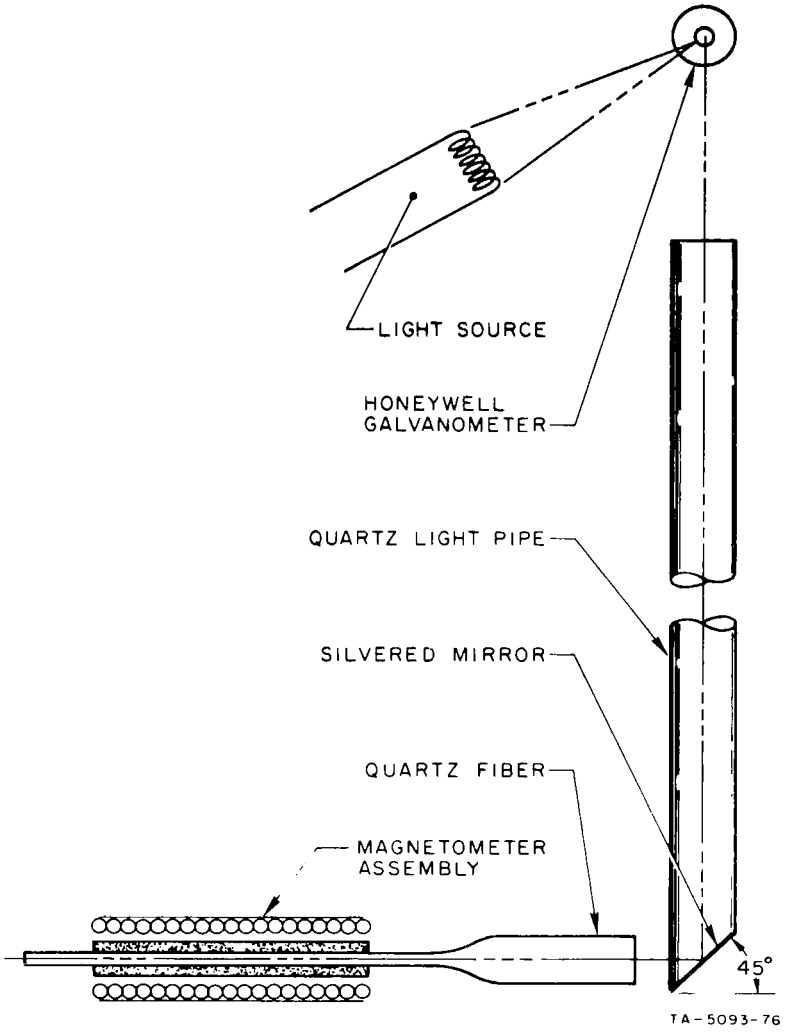

FIG. 17 OPTICAL MODULATION APPARATUS
FOR A QUANTIZED-FLUX MODULATOR

and circumferentially through the modulator material. We since have learned that these cracks are formed by thermal etching.[21] This process occurs when a material is deposited onto a hot surface. The etching effectively opened the modulator along the generator in numerous places; thus the only effect of switching was the Meissner effect due to flux being expelled from the walls. The walls were extremely thin, and we did not have sufficient sensitivity in our circuit to see this Meissner-effect signal.

Our hypothesis of thermal etching has been confirmed recently by further experiments at Stanford University, where superconducting modulators have been made successfully on quartz fibers.[22] In this case, the deposition procedure was designed very carefully to prevent overheating of the quartz during evaporation. The boat that contained the metal being evaporated was optically shielded, with room temperature shields placed between the boat and the modulator except for a small hole through which the evaporated metal could pass. Further, the modulator was mounted on a movable fixture so that it could be rotated over the evaporation boat for a few seconds, moved away and allowed to cool, then returned--with this process continuing until a sufficient superconductor thickness was built up. The modulators constructed at Stanford University still were electrically heated, having an electrical resistive film deposited before the superconducting film.

During our attempts to construct an optically heated modulator circuit, we tested several dry tantalum capacitors (Sprague type 150D*) at liquid helium temperatures. We anticipated using these to tune the output circuit of the modulator at liquid helium temperatures, thereby increasing the Q of the circuit. In general, the capacitance dropped to about one-sixth its room temperature value, and the power dissipation increased by an order of magnitude when the capacitor was cooled to liquid helium temperatures. We tried these capacitors because of the very large capacitance available in a small physical size. We now understand that other types of capacitors, such as the tantalum-mylar capacitor, work very well at helium temperatures with no significant change in capacitance or dielectric loss. These were not studied in our experiments.

---

* Sprague Products Company, 99 Marshall Street, North Adams, Mass.

VIII APPLICATIONS OF THE dc JOSEPHSON EFFECT*

A brief discussion of the theory of Josephson junctions was given in Section II. We now consider several techniques for constructing junctions and describe five device applications of these junctions.

The first Josephson junctions were built by evaporating a superconducting ground plane, covering this with an evaporated dielectric layer, and evaporating another superconductor onto the dielectric. These circuits were very difficult to build because the dielectric layer between superconductors had to be 10 or 20 Å thick with few or no pinholes that would allow the two superconducting layers to make direct contact. Due to the construction difficulties with circuits of this nature, we initially considered the Josephson effect to be an impractical method for constructing a useful magnetometer for field application. Recently, several developments in construction technique have changed considerably the complexity of building reproducible, stable Josephson junctions. The first was a technique developed at the Ford Scientific Laboratory called the point contact Josephson junction.[23] This consists essentially of a superconducting ground plane that is allowed to oxidize slightly; a sharp pointed superconductor then is pressed into this ground plane at helium temperatures until the proper tunneling characteristics are observed. This junction is probably a weak link tunnel where there is physical contact between superconductors but over a very small cross section area.

Another and even simpler Josephson junction can be built by a technique described by Clarke.[5] This technique consists of taking a small diameter superconducting wire, such as tantalum or niobium, allowing the surface to oxidize to a depth of approximately 20 Å, and then casting a "glob" of radio solder about the wire. The solder is superconducting as is the core of the wire, and the oxide layer on the surface of the wire forms the junction dielectric. Figure 18 is a schematic diagram of a typical tunneling junction built in this manner. The characteristics of

---

* The applications of the dc Josephson effect described in this section were given in a paper presented at the International Conference on Cryogenic Engineering in Kyoto, Japan, during April 1967.[8]

the junction are measured by passing a current through the niobium wire, across the dielectric barrier, and then through the solder. The voltage is then measured across the dielectric barrier. This junction has several distinct advantages over planar evaporated junctions of the type discussed earlier.

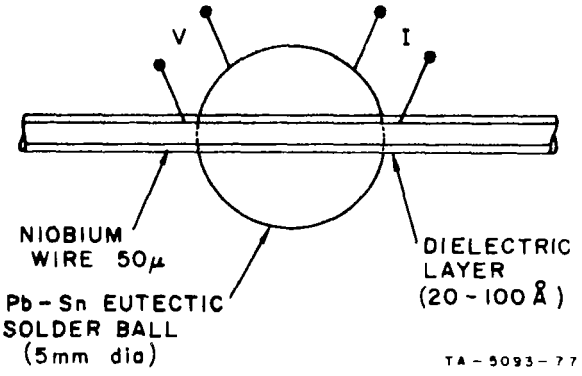

FIG. 18 CONSTRUCTION OF A SLUG TYPE JOSEPHSON JUNCTION

The first advantage of the Clarke junction is that the magnetic field linking the dielectric barrier is controlled by varying the current that passes directly through the superconducting center wire. This current produces a circumferential field that links the area between the two superconductors. A second advantage is that the solder glob tends to shield the dielectric barrier from external field changes.

Clarke[5] has given a very complete description of the use of this circuit to measure voltages of the order of 10^{-14} Vdc and magnetic fields of approximately 10^{-8} G. We repeated the experiments that Clarke reported and found that it is quite easy to build circuits that would give the same results.

The detailed characteristics of junctions of this type are not yet well understood because the nature of the junction is very complicated, possibly consisting of numerous weak links through the dielectric barrier. In many of our experiments, we did observe interference effects that seem to indicate that the junction actually divided into two junctions separated by a length approximately equal to the length of the wire covered by the solder glob, thus giving fairly high resolution interference patterns. By resolving a small fraction of one of these interference patterns, we were able to measure currents of less than 10^{-7} amp through the 10^{-8}-henry inductance of the center wire.

We have used this Clarke slug tunneling junction in the following five experimental systems:

1. A low impedance ammeter as discussed above.

2. A magnetometer for measuring changes in magnetic field (Figure 19). Field changes of less than 5×10^{-7} G were easily resolved with this device.

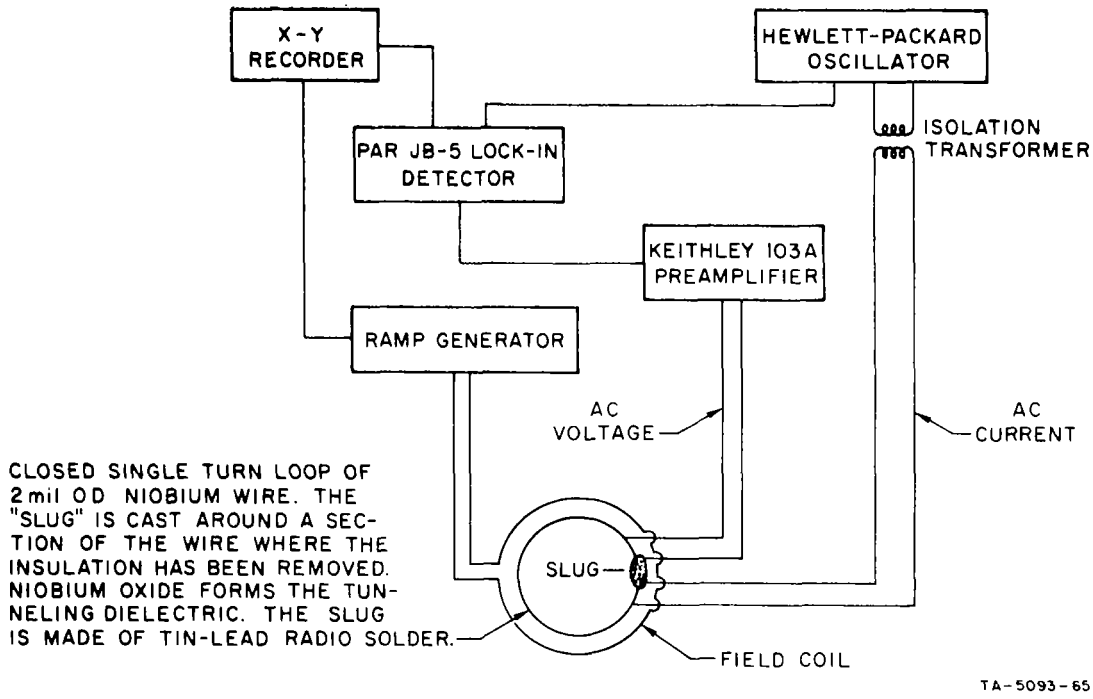

FIG. 19 JOSEPHSON JUNCTION MAGNETOMETER

3. A magnetic field gradiometer (Figure 20), which consists of two one-turn circular loops approximately 5 cm in diameter, wound in opposite directions on a form. The loops are in parallel planes and separated by about 20 cm. They are connected with 0.05-mm-diameter niobium wire, and a tunneling junction is cast on one of these connecting wires. A field change common to both loops does not produce any net flux change through the closed superconducting circuit since the loops are counterwound. A field gradient, on the other hand, does produce a net flux change through the circuit, which causes a persistent current to flow. A measure of this current, using the slug detector, is then a

measure of the field difference between the two loops. This circuit only measures the changes in field gradient that occur after the circuit becomes superconducting. Field gradients of less than 10^{-8} G cm have been measured with this system.

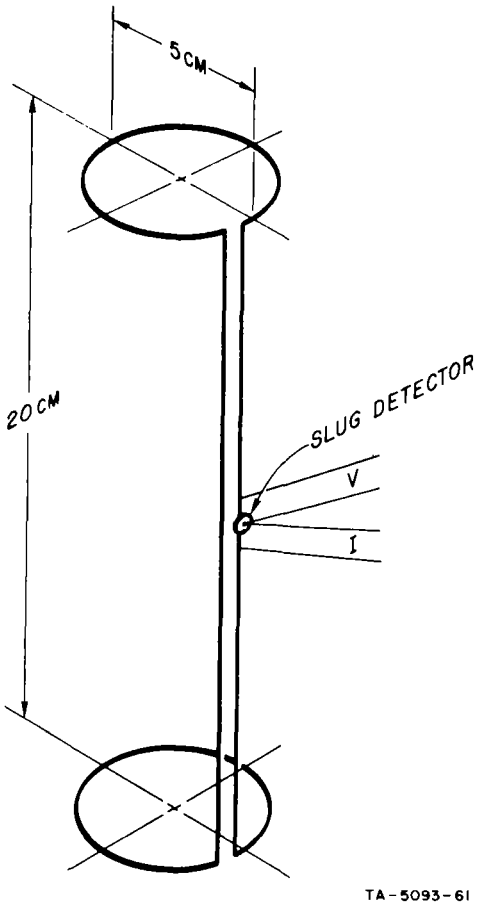

FIG. 20 JOSEPHSON JUNCTION MAGNETIC GRADIOMETER

4. A displacement measuring instrument (Figure 21), which is simply a magnetic piston (a superconducting tin bar in our experiment) that is inserted into a closed superconducting loop connected in series with a slug-type Josephson junction. Movement of the magnetic piston produces an attempted flux change through the closed loop, which causes a persistent current to flow. This current is a function of the piston displacement and the applied magnetic field. The slug is used to measure this current, calibrated in terms of the linear displacement of the magnetic piston. Preliminary experiments have proved that the technique is feasible

and that displacements of less than 1,500 Å can be measured easily. In these experiments, the sensitivity was limited only by the resolution of the method used to move the magnetic piston, and we expect that much better sensitivity can be realized.

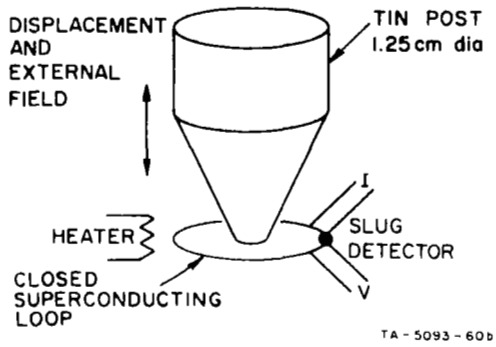

FIG. 21 JOSEPHSON JUNCTION DISPLACEMENT INDICATOR

5. A very sensitive system for measuring the static magnetic susceptibility of samples at liquid helium temperatures. This system is very similar to the displacement measuring system described above. The one-turn coil of the displacement measuring system is replaced by a long solenoid that will couple efficiently to the entire sample. The sample is inserted in the coil while a heat switch keeps part of the coil above its critical temperature and the desired external field is applied. The coil then is returned to the superconducting state, and the sample is removed completely from the coil so that no flux from the sample can couple to the coil. The total current induced in the coil, measured with the Josephson junction, is directly proportional to the magnetic susceptibility of the sample.

The above circuit (item 5) has been used in preliminary experiments to study both the Meissner effect and the time dependence of the flux motion in the heavy wall Meissner modulators used in our magnetometer experiments. In these experiments, the modulator was mounted inside a snugly fitting pickup coil and, instead of moving the modulator physically into and out of the coil, we cycled it above and below its transition temperature with direct current passing through the resistive film heater. One objective of these experiments was to determine if the Meissner effect was exactly reproducible from cycle to cycle, but the system was not sensitive enough to measure the Meissner effect at very low field levels where fluctuations are most likely to occur.

We were also interested in determining the time dependence of this flux exclusion process. The sensitivity of our system was not adequate to detect individual flux quanta, although minor refinements (both in the coupling to the sample and the electronic readout equipment) should make this possible. The time response of the system was limited to about 0.1 second by the detector, and a pen recorder was used to record the signal from the tunneling junction. We observed that the superconducting-to-normal transition of the modulator occurred considerably faster than this time constant, while the normal-to-superconducting transition occurred in times varying from 1 to 10 seconds, depending on the field at the modulator.

Figure 22 shows a typical normal-to-superconducting, superconducting-to-normal transition plot taken with this system. These time measurements of the normal-to-superconducting transition are in very good agreement with the work of DeSorbo,[24] where the normal-to-superconducting transition was studied using magneto-optic techniques.

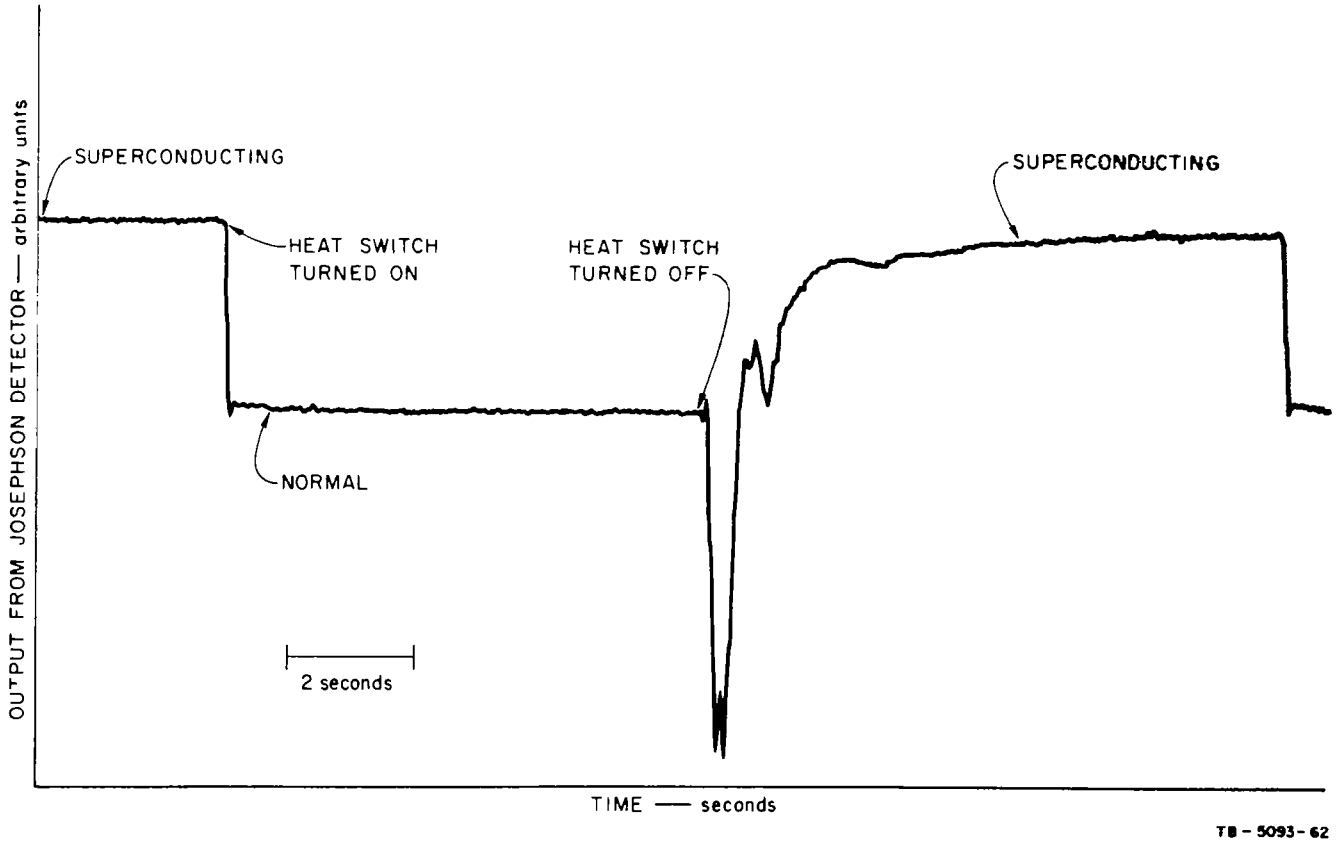

FIG. 22 SUPERCONDUCTING TRANSITIONS OF A MEISSNER MODULATOR

IX CONCLUSIONS AND RECOMMENDATIONS

During our research program, we discovered better, easier, or more logical ways to achieve the stated objectives. Thus this chapter is devoted to the results of our research and recommendations for experimental investigations that would increase understanding of the superconducting devices studied.

A. Magnetic Shield

The superconducting magnetic shield described in Section III was studied extensively during the many experiments in which it was used. In general, the shield was completely satisfactory for its designed purpose, i.e., providing a stable low magnetic field environment for magnetometer tests. During these tests, we conceived several ideas for a new shield that would reduce the helium boil-off rate of the shield assembly and make construction easier. We recommend the latter design over the one we built in this research (see Section III).

The new shield design is shown in Figure 23. Helium boil-off rate could be reduced from 1 liter/hour to less than 1 liter/day. The significant features of this design are: (1) all components are placed in the same vacuum space so that heat leaks are minimized, (2) all low temperature demountable vacuum seals are eliminated, and (3) the room temperature access can pass completely through the shield Dewar. The detailed placement of components shown in Figure 23 is for illustrative purposes only. Such features as efficient use of the cold helium boil-off vapor, radiation shielding, transfer lines, possible omission of the liquid nitrogen shield, etc., were not considered in this preliminary design suggestion.

B. Meissner-Effect and Quantized-Flux Magnetometers

The quantized-flux and Meissner-effect magnetometers could be used to resolve magnetic field changes of the order of 10^{-6} G. The resolution was limited by noise from the superconducting modulator that was due, as indicated by the experiments discussed in Sections V and VI, primarily to the thermal and magnetic environment at the modulator. From our studies of the Meissner-effect modulator, we can conclude (for cylindrical modulators at least) that the resolution of axial magnetic fields is limited by the transverse field at the modulator.

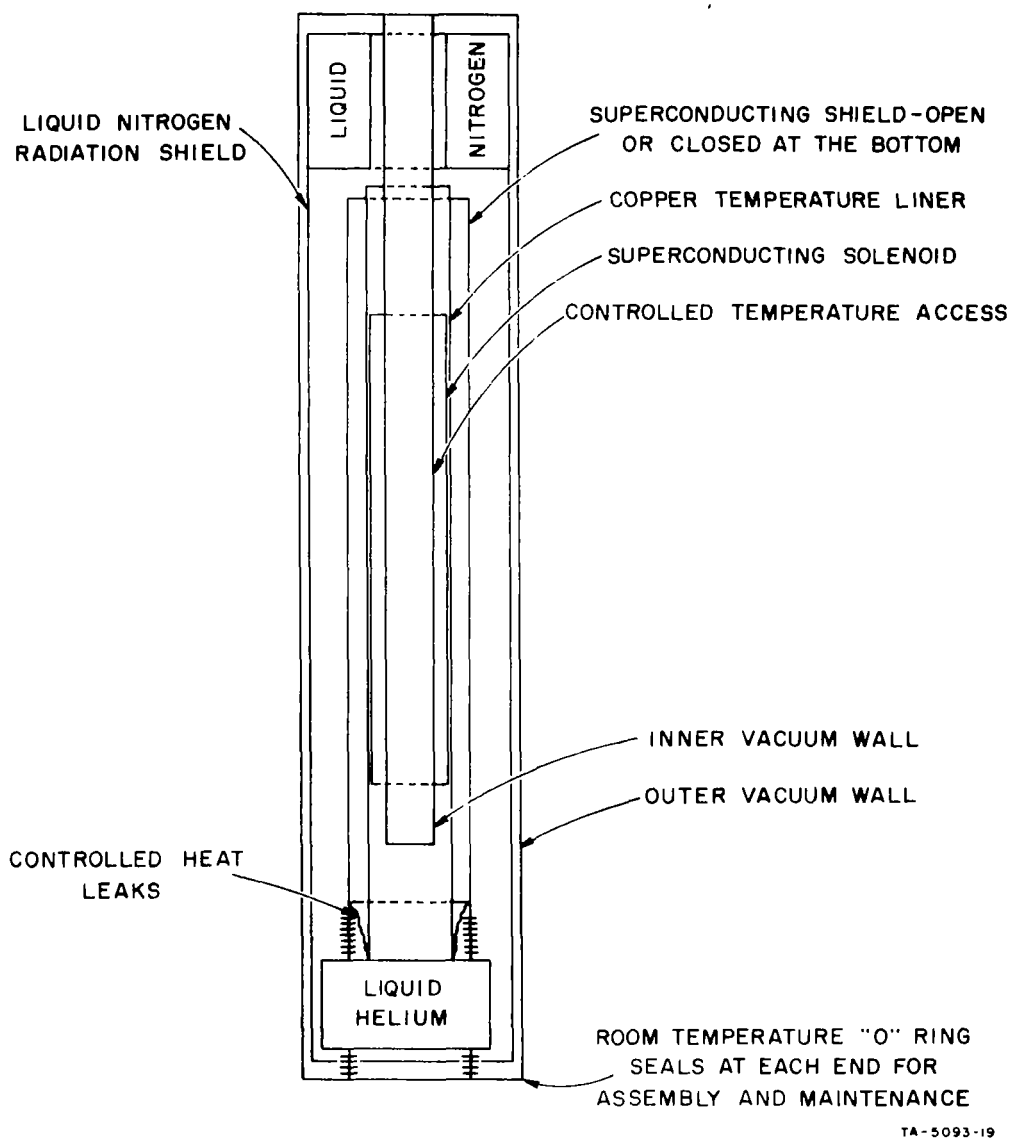

FIG. 23 PROPOSED DESIGN FOR A SUPERCONDUCTING MAGNETIC SHIELD

Our studies also indicated that all of the noise observed was related to switching the modulator between the normal and superconducting state. Therefore, we recommend that further research on Meissner-effect or quantized-flux devices should have as one of its major objectives a detailed study of noise inherent to the intermediate state of superconductors. It is difficult to evaluate the applications of these devices without additional information about this intrinsic noise.

The following discussion describes several techniques that may improve modulator performance and that would be useful in studying the noise problems discussed above. These studies were not made during this research project because of the extreme difficulty in obtaining reproducible results with the cylindrical modulators investigated. We now feel that enough has been learned about the dependence of the modulator output on the thermal and magnetic environment that these suggested extensions of the research would be both practical and informative.

The magnetometer circuits (Meissner effect and quantized flux) exhibited very similar characteristics and can be dealt with together. Magnetometer performance probably could be improved if the operating frequency could be increased without decreasing the modulation efficiency or increasing the noise. Calculations and our experiments have indicated that the modulation efficiency is most seriously reduced by thermal considerations and eddy-current flux-motion phenomena. The thermal problems are (1) optimizing the thermal relaxation time of the modulator material, (2) reducing the thermal impedance between the modulator and the temperature sink (usually the liquid helium bath), and (3) eliminating temperature gradients or fluctuations at the modulator. This particularly applies to bubble formation at the surface of the modulator.

The thermal relaxation time is related closely to the eddy-current damping, i.e., most materials with high thermal conductivity leading to short thermal relaxations times also have high normal state electrical conductivity, which results in reduced modulation efficiency. A study of alloys and modulator geometries, other than cylindrical ones, may result in overall improvement of these two effects.

A technique that may improve the modulation efficiency and reduce temperature fluctuations due to boiling, etc., is shown in Figure 24. The modulator is cooled from the inside out by conduction along the center copper wire, thereby maximizing the amount of flux excluded per cycle. The probable difficulty with this method of cooling is that eddy-current damping in the center copper wire plus thermal response would limit the operating frequency as discussed below.

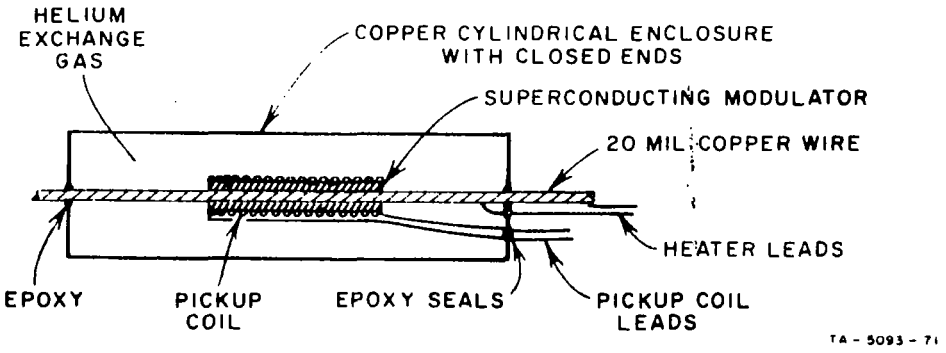

FIG. 24 COOLING OF THE MEISSNER-EFFECT MAGNETOMETER FROM THE INSIDE OUT

It should be realized that the copper wire that forms the center heater conductor of our modulators also introduces eddy-current damping. The skin depth for copper at 4.2°K and 10 kHz is only about 0.06 mm, so this effect is not negligible. The copper wire may be replaced with a dielectric such as quartz; the heater would then be evaporated on the quartz, insulated, and the modulator constructed as before. In future work, this technique should be investigated.

The eddy-current flux-motion problem seems to set the most serious limitations on modulator performance. This is especially true for the Meissner-type modulators. As discussed in Section VIII, the transition from normal to superconducting for a tin cylindrical modulator may take as long as several seconds.

The best way to solve the thermal impedance problem may be to use a modulator material whose critical temperature is less than the lambda point of liquid helium. Thus no boiling would occur, the uniform temperatures would be much easier to achieve. The quantized-flux modulator could be constructed of a very thin aluminum film whose critical temperature can be controlled in the range from about 1.2 to 2°K.

The critical temperature of bulk aluminum is 1.2°K; it is a difficult material to use in the Meissner-effect modulators due to the problem of maintaining this low temperature. In fact, there is no obvious choice of Meissner modulator material with a critical temperature less than 2.17°K (lambda point of He^4) that also exhibits an appreciable Meissner effect.

From the work of DeSorbo,[24] we conclude that the normal-state eddy-currents provide the major impedence to flux motion. We have considered several modulator geometries that should reduce the eddy-currents. The simplest geometry is a cylinder with several axial slits through its

walls. We attempted to cast one modulator with these axial slits but were unable to get the individual superconducting strips to bond to the modulator heater.

Another, and probably better, geometry would be multiple plane layers of superconductors, insulators, etc., built up to give a sufficient volume of superconducting material. A modulator of this type also would have a larger surface-to-volume ratio, possibly giving faster thermal response.

C. Josephson Junction Devices

In our opinion, the point contact and Clarke slug Josephson junctions are the most promising superconducting elements for general device development. These junctions work even after repeated cycling to room temperature in contrast to evaporated junctions, which generally do not survive a single temperature cycle. The junction characteristics often change after the junction has been cycled to room temperature, and this lack of stability is one of the major problems to be solved before tunnel junctions can be used in instrument development.

The superconducting tunnel junction operates without thermal cycling and therefore does not suffer from the intermediate state noise like that observed with the Meissner-effect and quantized-flux modulators. This is not to say that Josephson junctions are noise free. The tunnel junction is analogous in many ways to a Type II superconductor and would probably exhibit noise due to flux motion and temperature fluctuations. Several theoretical studies of shot noise in tunnel junctions have been reported recently,[25] but so far one cannot predict the magnitude of the noise spectrum.

We recommend a serious research effort to understand the noise in Josephson junctions and to understand how to make junctions with stable, reproducible, and predictable characteristics. These studies could have profound impact on the applications of superconductivity to instruments such as magnetometers with sensitivities as good as 10^{-12} G and voltmeters as sensitive as 10^{-18} Vdc.

Appendix A

MAGNETOMETER CIRCUIT ANALYSIS

The equivalent circuit diagram of the superconducting magnetometer is shown in Figure A-1. The modulator is represented by a time varying inductance, L(t), of the pickup winding, an emf generator, e_1, and the inductance, L_e, and resistance, R_e, experienced by the eddy currents in the modulator core when it is normal. (When the modulator core is superconducting, these eddy currents are replaced by superconducting shielding currents, which are taken into account by the bulk susceptibility, χ, of the modulator core.) The emf, e_1, is equal to $N\dot{\Phi}$, where $\dot{\Phi}$ is the time derivative of the flux switched in and out of the modulator by the heating and cooling of the core. The flux generated in the pickup winding by the current, i, is not included in Φ but is taken into account by the inductance, L. The resistance, R_1, is introduced into the magnetometer to prevent persistent currents in the primary. It is typically much smaller than $\omega(L+L_1)$, e.g., around 10^{-8} Ω. The transformer, which is entirely superconducting, provides impedance matching between the low impedance modulator and the high impedance of the preamplifier that amplifies e_o prior to the lock-in detector. (The preamplifier and lock-in detector are not shown in Figure A-1.) The resistance, R_2 (typically of the order of 0.05 Ω) is the resistance of the leads coming out of the cryostat. The capacitor, C, was at room temperature but could be placed in the liquid helium bath so that R_2 could be reduced to zero if desired. The resistance, R_L, is the input resistance of the preamplifier.

The circuit analysis to be given contains two major approximations for the sake of simplification; first, the eddy currents in the modulator core are not included; and second, the inductance, L(t), is assumed constant. The quality of these approximations has not yet been determined. It is important that this be done in the future. The second approximation eliminates an emf term, i dL/dt, and holds constant the coefficient, L, in the inductive voltage drop, L di/dt. These terms, which come from the time derivative of (Li), would greatly complicate the analysis because of their nonlinear character. Most of the experimental data of this report were taken for modulation frequencies in excess of 1 kHz, for which the amplitude of modulation was less than 1%. Under this condition, the percentage variation in L would also be small, and L in the term L di/dt will be very nearly constant. The other term, i dL/dt, also decreases with the percent modulation; however, the desired signal, $N\dot{\Phi}$, decreases for the

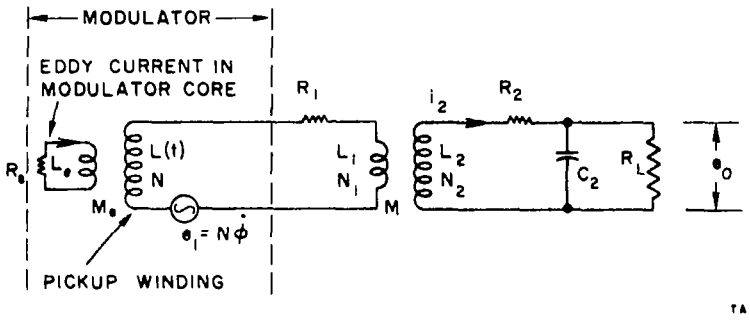

FIG. A-1 EQUIVALENT CIRCUIT OF THE MODULATED INDUCTANCE SUPERCONDUCTING MAGNETOMETER

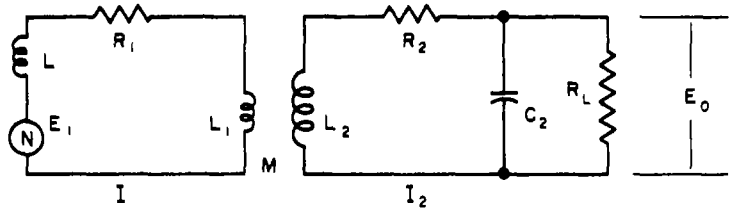

(a) FIRST STEP

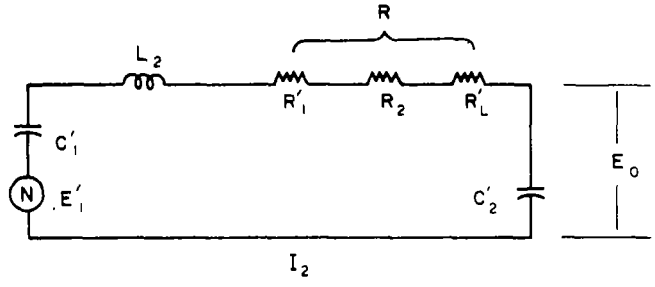

(b) SECOND STEP

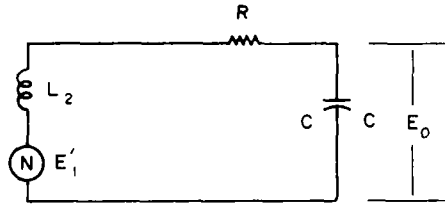

(c) THIRD STEP

TA-5093-78

FIG. A-2 REDUCTION OF EQUIVALENT CIRCUIT FOR ANALYSIS

same reason. Therefore, this linear analysis is only a crude approximation but is used for determining the values of the circuit quantities for lack of anything better.

The general method of optimization will be to compute e_o in terms of all the circuit quantities, determine the value of c_2 for proper tuning, and then maximize e_o as a function of L_1 and L_2. It will be assumed that R_1, R_2, and R_L are fixed by other considerations, although their effect on e_o can be examined from the equations to be derived. The voltage generator, e_1, is assumed to be known and its value computed later as a function of the B field to be measured by the magnetometer. The waveform of $e_1(t)$ is not necessarily sinusoidal; however, the high-Q output circuit will amplify only the fundamental Fourier component. Therefore, the fundamental Fourier coefficient will be introduced when e_1 is computed. For the purpose of analysis, the rms values of e_1 and e_o, E_1 and E_o, will be used. The circuit can now be redrawn as shown in Figure A-2(a). The primary is next reflected into the secondary circuit to obtain the circuit of Figure A-2(b). The reflected quantities are given by:[28]

$$E_1' = \frac{-j\omega E_1 M}{R_1 + j\omega(L+L_1)} \tag{A-1}$$

$$C_1' = \frac{R_1^2 + \omega^2 (L+L_1)^2}{\omega^4 M^2 (L+L_1)} \tag{A-2}$$

$$R_1' = \frac{R_1 \omega^2 M^2}{R_1^2 + \omega^2 (L+L_1)^2} \tag{A-3}$$

Since $R_1 \ll \omega(L+L_1)$ for the case being considered, we can write

$$E_1' = \frac{-ME_1}{L + L_1} \tag{A-4}$$

$$C_1' = \frac{L + L_1}{\omega^2 M^2} \tag{A-5}$$

$$R_1' = \frac{R_1 M^2}{(L+L_1)^2} \tag{A-6}$$

The values of C_2' and R_L' are given by

$$C_2' = C_2 \frac{1 + Q_L^2}{Q_L^2} \tag{A-7}$$

$$R_L' = \frac{R_L}{1 + Q_L^2} \tag{A-8}$$

where $Q_L = \omega C_2 R_L$. Since $Q_L \gg 1$ for the case being considered, we can write

$$C_2' = C_2 \tag{A-9}$$

$$R_L' = \frac{R_L}{Q_L^2} \tag{A-10}$$

The circuit can now be reduced to that of Figure A-2(c), where

$$R = \frac{R_1 M^2}{(L+L_1)^2} + R_2 + \frac{R_L}{Q_L^2} \tag{A-11}$$

$$E_1' = \frac{-ME_1}{L + L_1} \tag{A-12}$$

$$C = \frac{C_2}{1 + C_2(\omega^2 M^2 / L+L_1)} \tag{A-13}$$

The current, I_2, is given by

$$I_2 = \frac{-ME_1}{(L+L_1)(R+j\omega L_2[-j/\omega C])} \tag{A-14}$$

which is a maximum when the tuning condition

$$\omega L_2 = \frac{1}{\omega C} \tag{A-15}$$

is satisfied.

The value of C_2 required to maintain tuning can be obtained from Eqs. (A-15) and (A-13) to obtain

$$C_2 = \frac{1}{\omega^2 L_2 (1-[k^2 L_1/L+L_1])} \qquad \text{(A-16)}$$

where M has been replaced by $k\sqrt{L_1 L_2}$; k being the coupling coefficient of the transformer ($0 \leq k \leq 1$).

For C_2 tuned, I_2 can be written as

$$I_2 = \frac{-ME_1}{R(L+L_1)} \qquad \text{(A-17)}$$

E_0 is then given by

$$E_0 = \frac{-jI_2}{\omega C_2} \qquad \text{(A-18)}$$

or

$$E_0 = \frac{jME_1}{\omega RC_2 (L+L_1)} \qquad \text{(A-19)}$$

where $j = \sqrt{-1}$, i.e., E_0 is 90 degrees out of phase with E_1.

The total circuit Q can be defined as

$$Q = \frac{1}{\omega RC_2} = \frac{\omega L_2}{R} (1-[k^2 L_1/L+L_1]) \qquad \text{(A-20)}$$

so that E_0 becomes

$$E_0 = \frac{jME_1 Q}{L + L_1} \qquad \text{(A-21)}$$

Note that E_0 varies linearly with Q. If the circuit is not tuned (i.e., the capacity is eliminated), then Q in Eq. (A-21) can be replaced by 1. The effect of tuning is to amplify the output by a factor Q as might be expected.

The power output, E_o^2/R_L can be maximized by maximizing E_o, since R_L has been included in the derivation of E_o and is treated as constant. We now maximize E_o with respect to L_2 by writing Q of Eq. (A-21) in terms of L_2 by using Eq. (A-20), using the relation $M = k\sqrt{L_1 L_2}$, and by noting that $R_1 M^2/(L+L_1)^2 \ll R_2$ for the circuit being considered here $[R_1 M^2/(L+L_1)^2 \simeq 0.04\ R_2]$. Equation (A-11) then becomes

$$R = R_2 \left(1 + \frac{\omega^2 L_2^2 h^2}{R_2 R_L}\right) \tag{A-22}$$

where

$$h = \left(1 - \frac{k^2 L_1}{L + L_1}\right) \tag{A-23}$$

Thus E_o becomes

$$E_o = \frac{jE_1 kR_L L_1^{1/2} L^{3/2}}{\omega h(L+L_1)\left(\left[R_2 R_L/\omega^2 h^2\right]+L_2^2\right)} \tag{A-24}$$

This is of the form

$$E_o = \frac{bL_2^{3/2}}{d + L_2^2} \tag{A-25}$$

The maximum found by setting $\partial E_o/\partial L_2 = 0$ is

$$L_2 = \sqrt{\frac{3R_2 R_L}{\omega h}} \tag{A-26}$$

This optimum value for L_2 results in a Q given by

$$Q = \frac{1}{4}\sqrt{\frac{3R_L}{R_2}} \tag{A-27}$$

an R given by $R = 4R_2$, and an output voltage given by

$$E_o = \frac{jE_1 kL_1^{1/2} R_L^{3/4} 3^{3/4}}{4(L+L_1)\omega^{1/2} h^{1/2} R_2^{1/4}} \qquad \text{(A-28)}$$

We can now optimize E_o with respect to L_1 by using Eq. (A-23) for h, setting $\partial E_o/\partial L_1$ equal to zero, and solving for L_1. We obtain

$$L_1 = L/\sqrt{1-k^2} \qquad \text{(A-29)}$$

which is plotted in Figure A-3. Using this optimum value for L_1, we obtain

$$h = \sqrt{1-k^2}$$

and

$$E_o = \frac{jE_1 k(3R_L)^{3/4}}{4L^{1/2}\omega^{1/2} R_2^{1/4}(1+\sqrt{1-k^2})} \qquad \text{(A-30)}$$

If the value of Q given by Eq. (A-27) is too high from a circuit stability viewpoint, R_2 can be increased to hold Q fixed at the maximum tolerable value. The optimization of E_o with respect to L_1, using Eq. (A-21) and $M = k\sqrt{L_1 L_2}$, then becomes

$$L_1 = L \qquad \text{(A-31)}$$

Equation (A-29) gives nearly this same value for L_1 if $k \lesssim 0.5$ as shown in Figure A-3. For this type of optimum L_1, we obtain

$$E_o = \frac{jE_1 kQ}{2}\sqrt{L_2/L} \qquad \text{(A-32)}$$

The input voltage, e_1, can be written as

$$e_1 = N\dot{\Phi} = NB\dot{A}, \qquad \text{(A-33)}$$

where A is the effective normal area of the modulator core and B is the magnetic field being measured by the magnetometer. This assumes that the modulator length to diameter ratio is large enough to make the demagnetization factor nearly zero. The area, A, is given by

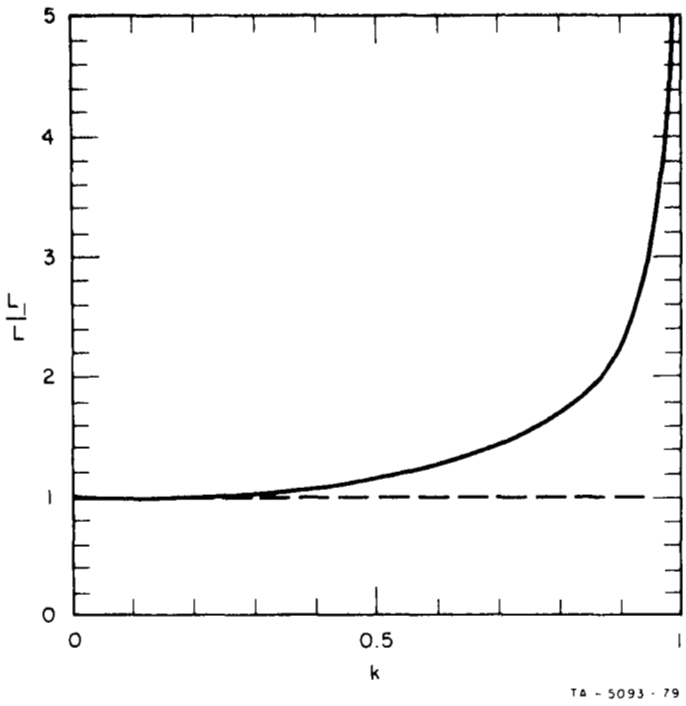

FIG. A-3 TRANSFORMER PRIMARY INDUCTANCE VERSUS COUPLING COEFFICIENT FOR MAXIMUM OUTPUT

$$A = A_c[1+ma\chi(t)] \tag{A-34}$$

where A_c is the area of the pickup winding, $a = A_m/A_c$, where A_m is the area of the modulator core, m is a factor ($0 \leq m \leq 1$), which accounts for the Meissner ratio and the hole of the core if there is one, and $\chi(t)$ is the average effective susceptibility of the modulator core. The thermal modulation causes χ to vary between 0 and -1 as the core goes from the normal to the superconducting state. The voltage, e_1, then becomes

$$e_1 = NBMA_m\dot{\chi} \tag{A-35}$$

The fundamental of $\dot{\chi}$ can be written as

$$\dot{\chi}_1 = \omega b_1 \cos \omega t, \tag{A-36}$$

where b_1 is the fundamental Fourier coefficient. E_1 then becomes

$$E_1 = \frac{-NBmA_m \omega b_1 j}{\sqrt{2}} \tag{A-37}$$

The inductance L in MKS units is given approximately as

$$L \simeq \frac{\mu_o N^2 A_c}{\ell} \tag{A-38}$$

where ℓ is the length of the pickup winding. The approximation here assumes that L is the inductance of the pickup winding when it is normal. Actually, an average value somewhat less than this could be used.

Using these equations for E_1 and L and Eq. (A-30) for E_o, we obtain

$$E_o = \frac{BMaA_c^{1/2}\omega^{1/2} b_1 k\ell^{1/2} (3R_L)^{3/4}}{4\sqrt{2}\, R_2^{1/4}\mu_o^{1/2}(1+\sqrt{1-k^2})} \tag{A-39}$$

The output power, E_o^2/R_L, is then given by

$$P = \frac{B^2 fVQK}{\mu_o} \qquad \text{(A-40)}$$

where

$$Q = \frac{1}{4}\sqrt{\frac{3R_L}{R_2}} \qquad \text{(A-27)}$$

$$V = A_m \ell = \text{volume of modulator core}$$

$$f = \omega/2\pi$$

$$K = \frac{27\pi m^2 a b_1^2 k^2}{4(1+\sqrt{1-k^2})} \qquad \text{(A-41)}$$

Note that N has been canceled. This means that N is arbitrary and can be chosen on the basis of practical considerations such as the size and shape of the wire cross section for maximum coupling to the modulator core. Equation (A-40) states that the maximum power obtainable from the circuit of Figure A-2 is proportional to the field energy in the volume of the modulator core times Q times the frequency with which this field is switched in and out of the core. The power is proportional to the circuit Q because the resistance associated with the source of e_1 is very nearly zero. This means that we have a voltage generator, e_1, with an unlimited source of power. Therefore, as Q is increased, the output power increases, and more power is removed from the source of e_1. This power comes from the heater current supply that switches the superconducting modulator. The numerical value of K in Eq. (A-41) is not to be trusted because of the approximation that L(t) is constant.

The actual design of the circuit can now be made as follows:

1. Choose a preamplifier with high input resistance because E_o in Eq. (A-30) increases with R_L.

2. Make $R_1 \ll R_2(L+L_1)^2/M^2$ so that it contributes little to circuit loss [see Eq. (A-11)].

3. Make R_2 as small as possible, except do not allow Q from Eq.(A-27) to become too large for good circuit stability. If necessary, C can be placed in the liquid helium bath and R_2 made very small.

4. Choose N convenient for obtaining good coupling to the flux in the modulator core.

5. Choose a modulator size. This is not straightforward since the maximum frequency of modulation is related to the size of the modulator. This then fixes L.

6. Make $L_1 \simeq L$ [see Eqs. (A-29) and (A-31)].

7. Choose ω as high as possible to obtain a significant percentage modulation. Note that Eq. (A-39) contains $\omega^{1/2}$ in the numerator.

8. Choose $k \simeq 0.9$, an easily obtainable value for a transformer made of close fitting solenoidal windings. Note that as k approaches unity, both L_2 and L_1 (for maximum output voltage) go to infinity. Therefore, it is not advantageous to make k greater than about 0.9.

9. Compute L_2 from Eq. (A-26).

10. Compute C_2 from Eq. (A-16).

It must be reiterated that this analysis makes two crude approximations that have not yet been evaluated, i.e., the eddy-currents in the modulator core are not included, and the inductance, L(t), is assumed constant.

Appendix B

CALCULATIONS OF SKIN DEPTH AND THERMAL RELAXATION TIME FOR SUPERCONDUCTING MODULATORS

The electrical skin depth,[27] δ, in millimeters is given by

$$\delta = \frac{2 \times 10^{-3}}{\mu_o \sigma \omega} \qquad \text{(B-1)}$$

where $\mu_o = 4\pi \times 10^{-7}$ henrys/m
σ = electrical conductivity = $1/\rho$
ρ = electrical resistivity
$\omega = 2\pi f$
f = frequency in Hz

$$\therefore \delta = 0.56\ \rho/\mu_o f \qquad \text{(B-2)}$$

The calculations were done for f = 10,000 Hz for tin, indium, mercury, lead, and copper. The electrical resistivity just above the critical temperature was used in all cases. The resistivity at 4.2°K was used for copper. Table B-1 gives the results of the skin depth calculation.

Table B-1

ELECTRICAL SKIN DEPTH
AT A FREQUENCY OF 10,000 Hz

Material	Electrical Resistivity, ρ (Ωm)	Electrical Skin Depth, δ (mm)
Tin	11.5×10^{-10}	0.169
Indium	1.7×10^{-11}	0.026
Mercury	5.3×10^{-10}	0.115
Lead	1.6×10^{-10}	0.063
Copper	1.7×10^{-10}	0.065

The thermal relaxation time for the superconducting modulators has been approximated by calculating the time constant in the heat diffusion equation

$$\dot{Q} = \exp[-A(K/c\rho\ell^2)] \qquad \text{(B-3)}$$

for the modulator material in the normal state just above the critical temperature. In this equation

A = constant
K = thermal conductivity in $w/cm^{\circ}K$
C = heat capacity in $joules/gm^{\circ}K$
ρ = density in gm/cm^3
ℓ = length of thermal path in cm
T = temperature in $^{\circ}K$.

The values for K and C used in these calculations were taken from Reference 28. The relaxation time is then

$$\tau = \frac{1}{\pi^2} \frac{c\rho\ell^2}{K} \qquad \text{(B-4)}$$

For a tin rod 1 cm long that is heated at one end and cooled at the other, we find

$$\tau = \frac{(2.0\times10^{-4}\ j/gm^{\circ}K)(7.3\ gm/cm^2)(1\ cm)^2}{\pi^2(25\ w/cm^{\circ}K)} \qquad \text{(B-5)}$$

$$\tau = 5.91 \times 10^{-6}\ \text{sec}$$

The modulator geometry used in our experiments was a hollow cylinder of wall thickness Δ. Assuming that the thermal pulse propagates from the inner wall of the cylinder (the heat source) to the outer wall (the heat sink) along a radial direction, the length used in calculating the relaxation time is the wall thickness. Thus

$$\tau = \frac{1}{\pi^2} \frac{c\rho\Delta^2}{K} \qquad \text{(B-6)}$$

Calculations were done for a cylinder with 0.5 mm ID by 1.25 mm OD for various modulator materials. The results are shown in Table B-2.

Table B-2

THERMAL RELAXATION TIMES
FOR FIVE POSSIBLE MODULATOR MATERIALS

Material	Relaxation Time, τ (sec)
Tin	8.0×10^{-9}
Indium	7.6×10^{-7}
Mercury	9.3×10^{-6}
Lead	1.9×10^{-6}
Copper	1.5×10^{-8}

From these estimates of the thermal relaxation time, it is clear that modulators operating at frequencies as low as 10 to 20 kHz should not be limited by the thermal response.

REFERENCES

1. Kerwin, W.J., R.M. Munoz, and J.M. Prucha, Proceedings of the IEEE 17th Annual National Aerospace Electronics Conference, Dayton, Ohio (1965) p. 73

2. Munoz, R., "The Ames Magnetometer," 1966 National Telemetering Conference Proceedings

3. Sonett, C.P., "Modulation and Sampling of Hydromagnetic Waves," COSPAR-URSI Meeting, Buenos Aires, May 1965

4. Deaver, Jr., B.S. and W.S. Goree, "Some Techniques for Sensitive Magnetic Measurements Using Superconducting Circuits and Magnetic Shields," Rev. Sci. Instr. 38, 311 (1967)

5. Clarke, J., "A Superconducting Galvanometer Employing Josephson Tunneling," Phil. Mag. 13, 115 (1966)

6. Goree, W.S., Progress Report No. 13 on Contract NAS 2-2088, submitted by SRI to NASA-Ames, August 23, 1965, NASA CR 73156, 1965

7. Goree, W.S., Cryogenic Magnetometer Development, Midterm Report - October 1965 on Contract NAS 2-2088, submitted by SRI to NASA-Ames, NASA CR 73157, 1965

8. Goree, W.S. and Troy W. Barbee, Jr., "Sensitive Instruments Using Superconducting Properties," paper presented at the International Cryogenic Engineering Conference, Kyoto, Japan, April 10-14, 1967. Conference proceedings to be published

9. Jaklevic, R.C., J. Lambe, A.H. Silver, and J.E. Mercereau, "Quantum Interference Effects in Josephson Tunneling," Phys. Rev. Letters 12, 159 (1964) and "Quantum Interference from a Static Vector Potential in a Field-Free Region," ibid. 12, 274 (1964); J.E. Zimmerman and J.E. Mercereau, "Quantized Flux Pinning in Superconducting Niobium," ibid. 13, 125 (1964)

10. Langenberg, D.N., D.J. Scalapino, and B.N. Taylor, "Josephson Effects," Sci. Amer. 214, 30 (1966)

11. Anderson, P.W., "The Josephson Effect and Quantum Coherence Measurements in Superconductors and Super Fluids," to be published in Progress in Low Temperature Physics, ed., C.J. Gorter

12. Forgacs, R.L. and A. Warnick, "Lock-on Magnetometer Utilizing Superconducting Sensors," IEEE Trans. on Instr. and Measurement IM-5, 113 (1966)

13. Vant-Hull, L.L. and J.E. Mercereau, "Magnetic Shielding by a Superconducting Cylinder," Rev. Sci. Instr. 34, 1238 (1963)

14. Hildebrandt, A.F., private communication

15. Hildebrandt, A.F., "The Attainment of Zero Magnetic Field in a Superconducting Lead Shield," paper presented at the Symposium on the Physics of Superconducting Devices, Univ. of Virginia, April 1967, to be published

16. Deaver, Jr., B.S. and William M. Fairbank, "Quantized Magnetic Flux in Superconducting Cylinders," Proceedings of the Eighth International Conference on Low Temperature Physics, R.D. Davies, ed. (Butterworths Scientific Publications, Washington, 1963) p.116

17. Deaver, Jr., B.S., "Experimental Evidence for Quantized Magnetic Flux in Superconducting Cylinders," PhD thesis, Stanford University, 1962, p.17

18. Johnson, A.K. and P.M. Chirlian, "The Cryotron as an Ultra-Low-Noise Amplifier, Elimination of Excessive Cryotron Noise," IEEE Trans. on Magnetics MAG-2, 390 (1966)

19. Kwiram, A. and B.S. Deaver, Jr., "Observations of the Establishment of the Quantized Flux State in Times as Short as 10^{-5} Sec," Phys. Rev. Letters 13, 189 (1964)

20. Pierce, J.M., "A Persistent-Current Magnetometer with Novel Applications," paper presented at the Symposium on the Physics of Superconducting Devices, Univ. of Virginia, April 1967, to be published

21. Kingery, W.D., Introduction to Ceramics, John Wiley and Sons, Inc., New York, 1960, p.213

22. Holderman, L., Stanford University, private communication

23. Zimmerman, J.E. and A.H. Silver, "Macroscopic Quantum Interference Effects through Superconducting Point Contacts," Phys. Rev. 141, 367 (1966)

24. DeSorbo, W., "Precession of Flux in Superconducting Indium," Phil. Mag. 11, 853 (1965)

25. Scalapino, D.J., "Current Fluctuations in Superconducting Tunnel Junctions," and R.E. Burgess, "Quantization and Fluctuations in Superconductors," presented at Symposium on the Physics of Superconducting Devices, Univ. of Virginia, Charlottesville, April 1967. Proceedings to be published

26. Terman, F.E., Electronic and Radio Engineering, McGraw Hill Book Co., New York, 4th Edition, 1955, p.76

27. Panofsky, W. and M. Phillips, "Classical Electricity and Magnetism," Addison-Wesley Publishing Co., 1956, p.182

28. A Compendium of the Properties of Materials at Low Temperatures, Phase I, Part 2: Properties of Solids, October 1960, AD #249786 and Part II: Properties of Fluids, Solids, and Electrical Resistivity of Metallic Elements at Low Temperatures, December 1961, AD #272769